THE PLANT CELL

Research Article

Ustilaginoidea virens secretes a family of phosphatases that stabilize the negative immune regulator OsMPK6 and suppress plant immunity

Xinhang Zheng [iD] ,[1] Anfei Fang [iD] ,[1,2] Shanshan Qiu [iD] ,[1] Guosheng Zhao [iD] ,[1] Jiyang Wang [iD] ,[1] Shanzhi Wang [iD] ,[1] Junjun Wei [iD] ,[1] Han Gao [iD] ,[1] Jiyun Yang [iD] ,[1] Baohui Mou [iD] ,[1] Fuhao Cui [iD] ,[1] Jie Zhang [iD] ,[3] Jun Liu [iD] [1] and Wenxian Sun [iD] [1,4,*]

1   Department of Plant Pathology, the Ministry of Agriculture Key Laboratory of Pest Monitoring and Green Management, and Joint International Research Laboratory of Crop Molecular Breeding, Ministry of Education, China Agricultural University, Beijing, China
2   College of Plant Protection, Southwest University, Chongqing, China
3   Institute of Microbiology, Chinese Academy of Science, Beijing, China
4   College of Plant Protection, Jilin Agricultural University, Changchun, Jilin, China

*Author for correspondence: wxs@cau.edu.cn
X.Z., J.Z., and W.S. designed the experiments. X.Z., A.F., S.Q. G.Z., J.W., S.W., J.W., H.G., J.Y., B.M., and F.C. performed the experiments. X.Z., J. Z., J.L., and W. S. wrote the paper.
The author responsible for distribution of materials integral to the findings presented in this article in accordance with the policy described in the Instructions for Authors (https://academic.oup.com/plcell) is: Wenxian Sun (wxs@cau.edu.cn).

Abstract

Rice false smut caused by *Ustilaginoidea virens* is emerging as a devastating disease of rice (*Oryza sativa*) worldwide; however, the molecular mechanisms underlying *U. virens* virulence and pathogenicity remain largely unknown. Here we demonstrate that the small cysteine-rich secreted protein SCRE6 in *U. virens* is translocated into host cells during infection as a virulence factor. Knockout of *SCRE6* leads to attenuated *U. virens* virulence to rice. SCRE6 and its homologs in *U. virens* function as a novel family of mitogen-activated protein kinase phosphatases harboring no canonical phosphatase motif. SCRE6 interacts with and dephosphorylates the negative immune regulator OsMPK6 in rice, thus enhancing its stability and suppressing plant immunity. Ectopic expression of SCRE6 in transgenic rice promotes pathogen infection by suppressing the host immune responses. Our results reveal a previously unidentified fungal infection strategy in which the pathogen deploys a family of tyrosine phosphatases to stabilize a negative immune regulator in the host plant to facilitate its infection.

Introduction

Plants have evolved two major branches of innate immunity: pattern-triggered immunity (PTI) and effector-triggered immunity (ETI) (Jones and Dangl, 2006). PTI is activated by the recognition of pathogen- and damage-associated molecular patterns (P/DAMPs) by pattern recognition receptors (PRRs) located on the plasma membrane in plants (Jones and Dangl, 2006; Zipfel, 2014). Many effector molecules are secreted from phytopathogenic fungi into plant cells to suppress host immunity via such structures as the biotrophic interfacial complex (BIC), mycelia, and haustoria (Rafiqi et al., 2012). Specific recognition of certain effectors by

IN A NUTSHELL

Background: Rice commercial production is severely threatened by several important diseases including rice false smut. Once considered a minor disease, rice false smut caused by *Ustilaginoidea virens* has emerged as one of the most devastating rice diseases worldwide. *Ustilaginoidea Virens* is a unique flower-infecting fungal pathogen. The disease not only causes a significant yield loss (up to 40%), but also produces various types of mycotoxins that contaminate rice grains and deteriorate grain quality. *Ustilaginoidea Virens* secretes numerous effector proteins into host cells to promote infection. However, the molecular mechanisms by which these effectors contribute to *U. virens* pathogenicity are poorly understood, which hampers the development of effective management strategies for the disease.

Question: The rice fungal pathogen *U. virens* generates a large effector repertoire that is essential for its virulence and pathogenicity. In this study, we attempted to elucidate the biochemical functions of small cysteine-rich effector 6 (SCRE6), which is secreted by *U. virens*, and to determine how the effector suppresses rice immunity to promote infection.

Findings: The most important finding of our study is that SCRE6 and its homologs in *U. virens* constitute a family of protein tyrosine phosphatases with no canonical phosphatase motif. SCRE6 represents the first identified effector phosphatase in phytopathogenic fungi. SCRE6, which is secreted and translocated into rice cells during *U. virens* infection, interacts with and dephosphorylates the negative immune regulator MITOGEN-ACTIVATED PROTEIN KINASE 6 (OsMPK6) in rice. OsMPK6 dephosphorylation enhances its stability, thus inhibiting rice immunity.

Next steps: The most important next step is to investigate how OsMPK6 is degraded in vivo and how OsMPK6 phosphorylation promotes its degradation. The future challenge is to elucidate the molecular mechanisms by which OsMPK6 negatively regulates plant immunity in rice.

intracellular immune receptors in plants can trigger hypersensitive responses (HR), called ETI (Jones and Dangl, 2006; Rafiqi et al., 2012).

Protein phosphorylation is a common type of post-translational modification that can regulate plant immunity (Park et al., 2012). Many PRRs, including flagellin-sensitive 2 (FLS2), elongation factor-Tu receptor (EFR), and *Xanthomonas* resistance 21 (Xa21), have kinase activity and regulate defense signaling through protein phosphorylation (Park et al., 2012). When PRRs recognize PAMPs or DAMPs, plants activate a series of immune protein kinases, namely receptor-like cytoplasmic kinases, mitogen-activated protein kinase (MAPK) cascades, and calcium-dependent protein kinases (Wu and Zhou, 2013). Ensuing kinase-mediated phosphorylation plays a crucial role in regulating defense responses by altering the stability, activity, protein–protein interactions, and subcellular localization of target proteins (Xing et al., 2002; Bhaskara et al., 2019).

Protein phosphorylation is reversible, in a process mediated by protein phosphatases (Hunter, 1995; Luan, 2003). Protein phosphatases may be grouped into four families: phosphoprotein phosphatase; Mg^{2+}- or Mn^{2+}-dependent protein phosphatase/protein phosphatase 2C; phosphotyrosine phosphatase (PTP); and aspartate-dependent phosphatase (Hunter, 1995; Uhrig et al., 2013). Because protein phosphorylation is a type of post-translational modification crucial for plant defenses, dephosphorylation of immune-related proteins is thought to be a critical strategy for pathogen effectors to disarm plant immunity (Bhattacharjee et al., 2015). Indeed, a type III secreted effector (HopPtoD2/HopAO1) in *Pseudomonas syringae* pv. *tomato* possesses a tyrosine phosphatase domain at its C-terminus. In vitro purified HopPtoD2 has PTP activity, which requires the conserved catalytic Cys residue (Espinosa et al., 2003). As a tyrosine phosphatase, the effector reduces phosphorylation of multiple PRRs, including EFR and LIPOOLIGOSACCHARIDE-SPECIFIC REDUCED ELICITATION (LORE), a G-type lectin receptor-like kinase, in *Arabidopsis thaliana* (Macho et al., 2014; Luo et al., 2020). Specifically, HopAO1 dephosphorylates the phosphorylated Tyr600 in activated LORE, thus blocking subsequent immune signaling (Luo et al., 2020). Another type III effector in *P. syringae*, HopAI1, exhibits phosphothreonine lyase activity. HopAI1 interacts with and irreversibly dephosphorylates AtMPK3 and AtMPK6 to suppress plant immunity (Zhang et al., 2007). Intriguingly, the oomycete RXLR effector Pi04314 interacts with host protein phosphatase 1 catalytic isoforms to form holoenzymes, which presumably dephosphorylate the host proteins, thus promoting late blight disease (Boevink et al., 2016). However, no effector phosphatase has yet been reported in phytopathogenic fungi.

MAPK cascades regulate diverse biological functions and processes in plants (Hirt, 1997). During pathogen infection, MAPK cascades are activated as one of the earliest defense responses in plants. Generally, MAPKKKs first phosphorylate the two conserved Ser and/or Thr residues in the S/T-X5-S/T motif of MAPKKs, which transmit the signal to MAPKs by phosphorylating the Thr and/or Tyr residues in the TDY/TEY motif of MAPKs (Bi et al., 2018). MAPK cascades are

involved in multiple defense responses, such as the generation of reactive oxygen species (ROS), induced expression of defense marker genes, stomatal closure, and hypersensitivity (Meng and Zhang, 2013). In Arabidopsis, *mekk1*, *mkk1/mkk2*, and *mpk4* mutant seedlings exhibit elevated ROS production, constitutive expression of pathogenesis-related (*PR*) genes, and enhanced disease resistance, indicating that the typical MEKK1–MKK1/MKK2–MPK4 cascade negatively regulates plant innate immunity (Gao et al., 2008). Consistently, transgenic Arabidopsis plants that express a constitutively active MPK4 are more susceptible to *P. syringae* than the wild type (Berriri et al., 2012). OsMPK6 is a putative ortholog of MPK4 in Arabidopsis. The *osmpk6* mutant carries a R89K mutation in OsMPK6 that causes reduced kinase activity and results in increased resistance to *Xanthomonas oryzae* pv. *oryzae* (*Xoo*), in addition to elevated levels of ROS and *PR* gene expression. The *OsMPK6*-overexpressing transgenic lines are more susceptible to *Xoo* than the wild-type plants, indicating that OsMPK6 negatively regulates the resistance of rice to *Xoo* (Wang et al., 2021a). Interestingly, another study suggested that OsMPK6 could have the opposite function, by serving as both an activator and repressor in rice defense against *Xoo* (Yuan et al., 2007; Shen et al., 2010). The overexpression of *OsMPK6* promotes the accumulation of salicylic acid (SA) and jasmonic acid (JA) and induces the expression of JA- and SA-responsive genes (Yuan et al., 2007; Shen et al., 2010). In MAPK cascades, the intensity and duration of MAPK activation are balanced by phosphorylation and dephosphorylation (Bartels et al., 2010). Tyrosine and dual-specificity phosphatases function to dephosphorylate MAPKs and are the major negative regulators of MAPK activation (Bartels et al., 2010; Caunt and Keyse, 2013).

Ustilaginoidea virens, the causal agent of rice false smut, is a unique flower-infecting fungal pathogen. Typically, false smut balls are formed around unfertilized ovaries on rice panicles following host infection by *U. virens*. The disease has become one of the most important rice diseases globally, because it not only reduces rice grain yield but also diminishes grain quality due to the mycotoxins in false smut balls (Osada, 1995; Gao et al., 2012; Fan et al., 2016; Sun et al., 2020). An increasing number of virulence factors including multiple effectors have been recently demonstrated to be operative in *U. virens* (Sun et al., 2020). Indeed, a total of 421 conventional and non-conventional effectors have been predicted to exist in *U. virens* according to its updated genome (Zhang et al., 2021). Thirteen of these effectors were shown to induce necrosis or necrosis-like phenotypes in *Nicotiana benthamiana* (Fang et al., 2016). The secreted cysteine-rich effectors SCRE1 and SCRE2 suppress rice immunity and are both essential for *U. virens* infection (Fang et al., 2019; Zhang et al., 2020). Interestingly, a small peptide in SCRE1 containing a "Cys–Pro–Ala–Arg–Ser" motif is essential for its immune-suppressive activity (Zhang et al., 2020). Further, a Ser–Thr-rich glycosylphosphatidylinositol-anchored protein (SGP1) in *U. virens* is required for *U. virens*

virulence. Notably, a 22-amino-acid peptide (SNP22) in SGP1 functions as a PAMP, given that it is recognized by plants and therefore induces cell death, oxidative burst, and defense-related gene expression in rice (Song et al., 2021). Despite this progress, we still know surprisingly little about the molecular mechanisms underlying virulence functions of individual *U. virens* effectors.

In this study, we identified the virulence function of a small cysteine-rich effector 6 (SCRE6) in *U. virens*. The *scre6* knockout mutant has an attenuated virulence to rice. Ectopic expression of SCRE6 inhibits immune responses in rice. SCRE6 functions as a protein tyrosine phosphatase and dephosphorylates the negative defense regulator OsMPK6, thereby enhancing the accumulation of OsMPK6 and suppressing plant immunity. Therefore, through this work, we reveal that SCRE6 functions as an effector phosphatase in phytopathogenic fungi.

Results

SCRE6 is an essential virulence factor in *U. virens*

A small protein of 155 amino acid residues, SCRE6 (formerly called UV_7621) carries a predicted signal peptide (SP) and a nuclear localization signal (Supplemental Figure S1A) and has been demonstrated to suppress HR in *N. benthamiana* (Zhang et al., 2014). Here we generated *scre6* knockout mutants that were confirmed by the Southern blot analysis (Supplemental Figure S1B). The wild-type strain and two independent knockout mutants, Δ*scre6-34* and Δ*scre6-39*, were inoculated by injection into rice panicles of the false smut susceptible cultivar LYP9. The wild-type strain produced many more false smut balls on rice panicles than did *scre6-34* or *scre6-39* after inoculation (Figure 1A). The complementation strains Δ*scre6-34(SCRE6)* and Δ*scre6-39(SCRE6)* largely restored virulence of *U. virens* to rice (Figure 1A). These results indicate that SCRE6 is essential for *U. virens* virulence to rice.

Next, we performed a yeast protein secretion assay to verify the functionality of the predicted SP in SCRE6. The secreted invertase SUC2 catalyzes the splitting of an oligosaccharide into a monosaccharide to support yeast growth on raffinose-containing media (Jacobs et al., 1997; Fang et al., 2016). The *pSCRE6(SP)-SUC2* plasmid construct expressing the fusion protein of predicted SCRE6 SP and SP-lacking SUC2 was transformed into the yeast invertase-deficient strain YTK12. This transformed YTK12 strain grew well on both the complete minimal medium lacking tryptophan (CMD-W medium) and yeast extract peptone raffinose agar medium (YPRAA medium) with raffinose as the sole carbon source (Figure 1B). As a positive control, the YTK12 strain transformed with *pAvr1b(SP)-SUC2* also grew well on YPRAA medium. In contrast, the YTK12 strain transformed with the construct expressing SP-lacking SUC2 fused to the N terminus of the nonsecreted protein Mg87 grew on the CMD-W medium only, and not on the YPRAA medium. The results indicate that the predicted SP of SCRE6 is able
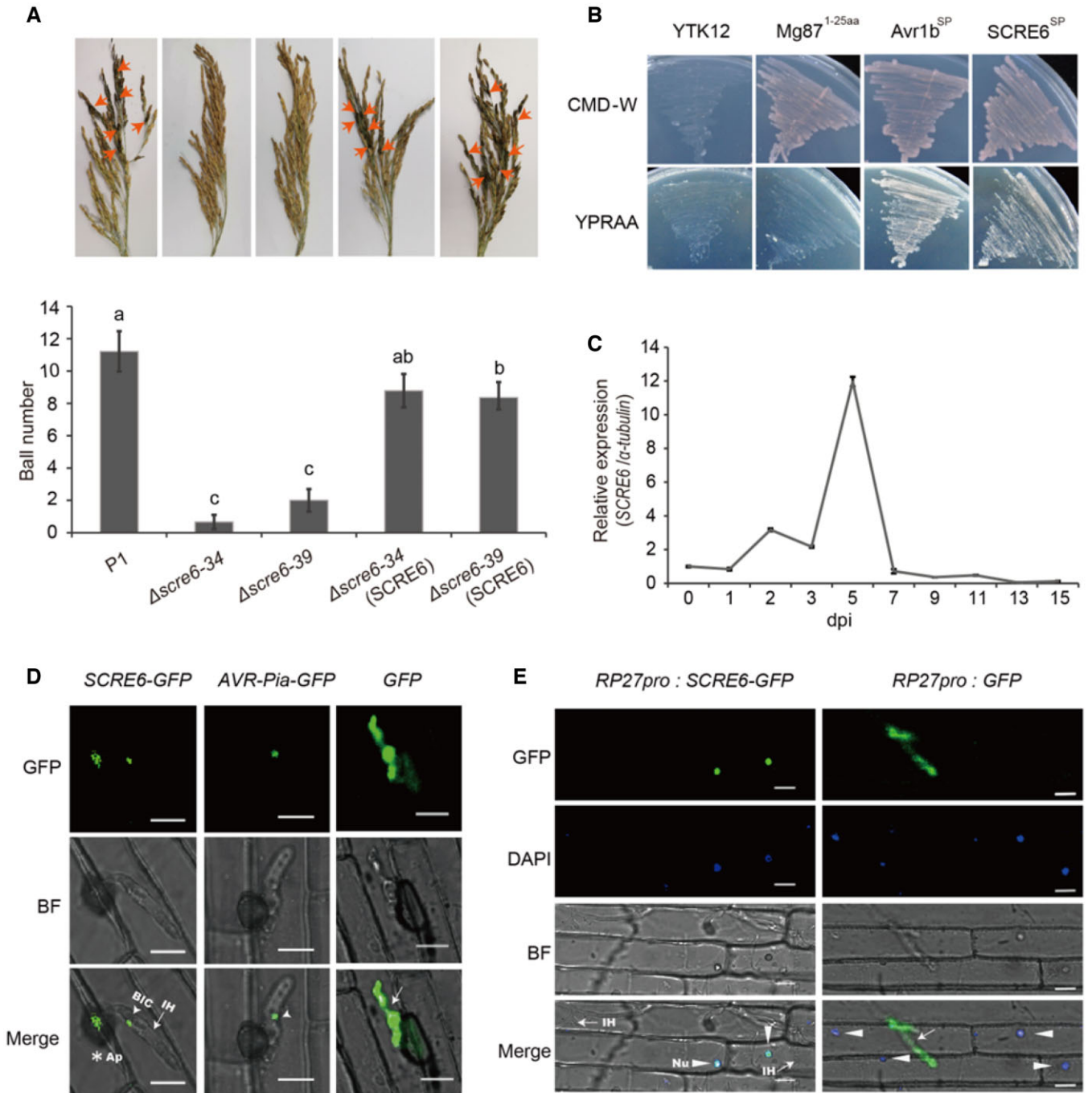
Figure 1 SCRE6 functions as an essential virulence effector in *U. virens*. A, The *scre6* knockout mutants generated fewer false smut balls on the inoculated rice panicles than did the wild-type and complementation strains. The wild-type P1, Δ*scre6-34*, Δ*scre6-39*, and complementation strains Δ*scre6-34(SCRE6)* and Δ*scre6-39(SCRE6)* were injected into young panicles of cultivar LYP9. Upper: representative rice panicles photographed at 4 weeks after inoculation with the indicated strains. Orange arrows indicate the false smut balls. Lower: the average number of false smut balls per inoculated panicle counted about 1 month post-inoculation. The bars are mean ± SE (n = 14, 9, 12, 14, and 14, respectively). Different letters (a–c) indicate significant differences in the number of false smut balls formed after inoculation on the wild-type, mutant, and complementation strains (one-way ANOVA least significant difference test, $P < 0.05$). B, Validation of the predicted signal peptide of SCRE6 by the yeast secretion assay. The invertase-deficient yeast strain YTK12 transformed with *pSCRE6(SP)-SUC2* grew well on CMD-W and YPRAA medium plates. The signal peptide of Avr1b and the first 25 amino-acid residues of Mg87 were expressed in frame with SUC2 without the signal peptide in yeast as positive and negative controls, respectively. C, Expression pattern of *SCRE6* during *U. virens* infection. The panicles of cultivar LYP9 were injection inoculated with *U. virens*. *SCRE6* expression was detected via quantitative RT-PCR at the indicated days post-inoculation (dpi) with α-tubulin serving as the internal reference gene. D and E, GFP signal resulting from the ectopic expression of SCRE6-GFP in *M. oryzae* accumulated in the BIC and in the epidermal cell nuclei of leaf sheaths at 30–36 h (D) and 42 h (E) after inoculation, respectively.

(continued)

to guide the secretion of SUC2. To determine whether SCRE6 is a genuine effector, we first examined the expression pattern of *SCRE6* during infection. *SCRE6* was transcriptionally upregulated after host infection with *U. virens*, peaking at 5-day post-inoculation (Figure 1C). Furthermore, we investigated the translocation of SCRE6 into host cells using the *Magnaporthe oryzae* Guy11 strain ectopically expressing SCRE6-GFP. When rice leaf sheath was inoculated with the engineered *M. oryzae* strain, green fluorescence was clearly observed to accumulate in the BIC at 30- to 36-h post-inoculation (Figure 1D). When the rice sheath was inoculated with *M. oryzae* expressing the cytoplasmic effector AVR-Pia-GFP (Qi et al., 2016) as a positive control, green fluorescence was also observed in the BICs. In contrast, green fluorescence was only discernible in invasive hyphae after rice sheaths were infected by GFP-expressing *M. oryzae* (Figure 1D). The data indicate that SCRE6 expressed in *M. oryzae* is translocated into rice cells during host infection. Moreover, green fluorescence from SCRE6-GFP was seen to accumulate in the nuclei of rice epidermal cells at 42-h post-infection (Figure 1E). Taken together, these results indicate that SCRE6 functions as an important virulence effector in *U. virens*.

SCRE6 interacts with OsMPK6 in vitro and in vivo

To explore how SCRE6 functions as a virulence factor, we performed yeast two-hybrid assays using SCRE6 as the bait and identified OsMPK6 as a candidate interactor from a rice mini-library which includes about 300 putative defense-related genes (Figure 2A). In luciferase complementation imaging (LCI) assays, a luminescence signal was detected when cLUC-SCRE6(-SP) and OsMPK6-nLUC were co-expressed in *N. benthamiana* leaves, indicating an in-planta interaction between SCRE6 and OsMPK6. In contrast, no signal was detected when cLUC-SCRE6(-SP) and OsMPK6-nLUC were co-expressed with nLUC and cLUC, respectively (Figure 2, B and C). Further, we demonstrated that His-OsMPK6 was co-pulled down with GST-SCRE6, but not with GST, when in vitro purified GST-SCRE6 and His-OsMPK6 were co-incubated with glutathione agarose beads (Figure 2D). Follow-up co-immunoprecipitation (co-IP) assays confirmed this interaction. OsMPK6-HA was co-expressed with SCRE6-FLAG and SCRE2-FLAG in rice protoplasts. Total proteins were extracted from the transfected protoplasts and subjected to immunoprecipitation with anti-FLAG affinity beads. As detected by immunoblotting, OsMPK6-HA co-immunoprecipitated with SCRE6-FLAG but not with SCRE2-FLAG (Figure 2E). Furthermore, SCRE6-FLAG was co-expressed with OsMPK1-HA, OsMPK6-HA, and OsMPK8-HA separately. Co-IP assays showed that SCRE6-FLAG was co-immunoprecipitated with OsMPK6-HA, yet not with

OsMPK1-HA or OsMPK8-HA (Figure 2F). Collectively, these assays indicate that SCRE6 directly and specifically interacts with OsMPK6, both in vitro and in vivo.

OsMPK6 phosphorylation promotes its proteosomal degradation

OsMPK6, as an important MAPK, could negatively regulate plant immunity (Wang et al., 2021a). Multiple protein kinases can regulate plant immunity by altering protein abundance, which is often mediated by phosphorylation (Mithoe and Menke, 2018). Accordingly, we investigated whether phosphorylation of OsMPK6 is involved in its degradation. First, we showed that OsMPK6-HA was rapidly degraded in *OsMPK6-HA*-transfected protoplasts at 2 h after treatment with cycloheximide (CHX, a protein synthesis inhibitor) and that this degradation was greatly inhibited by the 26S proteasome inhibitor MG132, but not by the cysteine proteinase inhibitor E64 or autophagy inhibitor Wortmannin (WM), suggesting that OsMPK6 is degraded through the ubiquitin proteasome system (Figure 3A). Further, in vitro kinase assays showed that OsMPK6 was strongly phosphorylated by constitutively active OsMKK1^{DD}, in which its phosphorylation residues Ser215 and Thr221 in the conserved S/T-X5-S/T motif had been replaced with two Asp residues (Supplemental Figure S2; Bi et al., 2018). Next, we determined whether OsMKK1-mediated OsMPK6 phosphorylation could affect its stability. OsMPK6 was degraded more rapidly when it was co-expressed with OsMKK1^{DD} than the kinase-inactive OsMKK1^{KR} whose Ser215 and Thr221 residues were replaced by Lys and Arg, respectively, in rice protoplasts (Figure 3B). Moreover, faster degradation of OsMPK6 occurred after the chitin treatment when compared with the mock treatment (Figure 3C). In addition, the phosphomimetic OsMPK6^{DD} and inactive OsMPK6^{AA} variants—in which Thr201 and Tyr203 in the conserved TEY phosphorylation sites were replaced with two Asp and Ala residues—were transiently expressed in rice protoplasts. In comparison with that of OsMPK6-HA, the degradation of inactive OsMPK6^{AA}-HA was delayed, while the phosphomimetic mutant OsMPK6^{DD} underwent a more rapid degradation after the CHX treatment (Figure 3D). The degradation of OsMPK6^{DD}-HA and OsMPK6-HA in the transfected protoplasts was substantially inhibited by MG132 (Supplemental Figure S3). These results indicate that OsMPK6 phosphorylation promotes its degradation in a proteasome-dependent way.

SCRE6 specifically reduces OsMPK6 phosphorylation

Given that OsMPK6 degradation was promoted by its phosphorylation, it is of interest to investigate whether SCRE6 could influence the phosphorylation of OsMPK6.

Figure 1 (Continued)
The engineered *M. oryzae* strains carrying the *RP27pro:SCRE6-GFP*, *RP27pro:AVR-Pia-GFP* or *RP27pro:GFP* constructs were inoculated onto rice leaf sheaths. These *M. oryzae*-infected leaf sheaths were observed using fluorescence microscopy. Rice sheaths were infected by the Guy11 strains expressing AVR-Pia-GFP and GFP to, respectively, serve as positive and negative controls. BICs, appressoria (Ap), invasive hyphae (IH), and nuclei (Nu) are indicated, respectively, by white arrowheads, asterisks, arrows, and triangles. The epidermal cell nuclei were stained with DAPI. Scale bar: 10 μM.
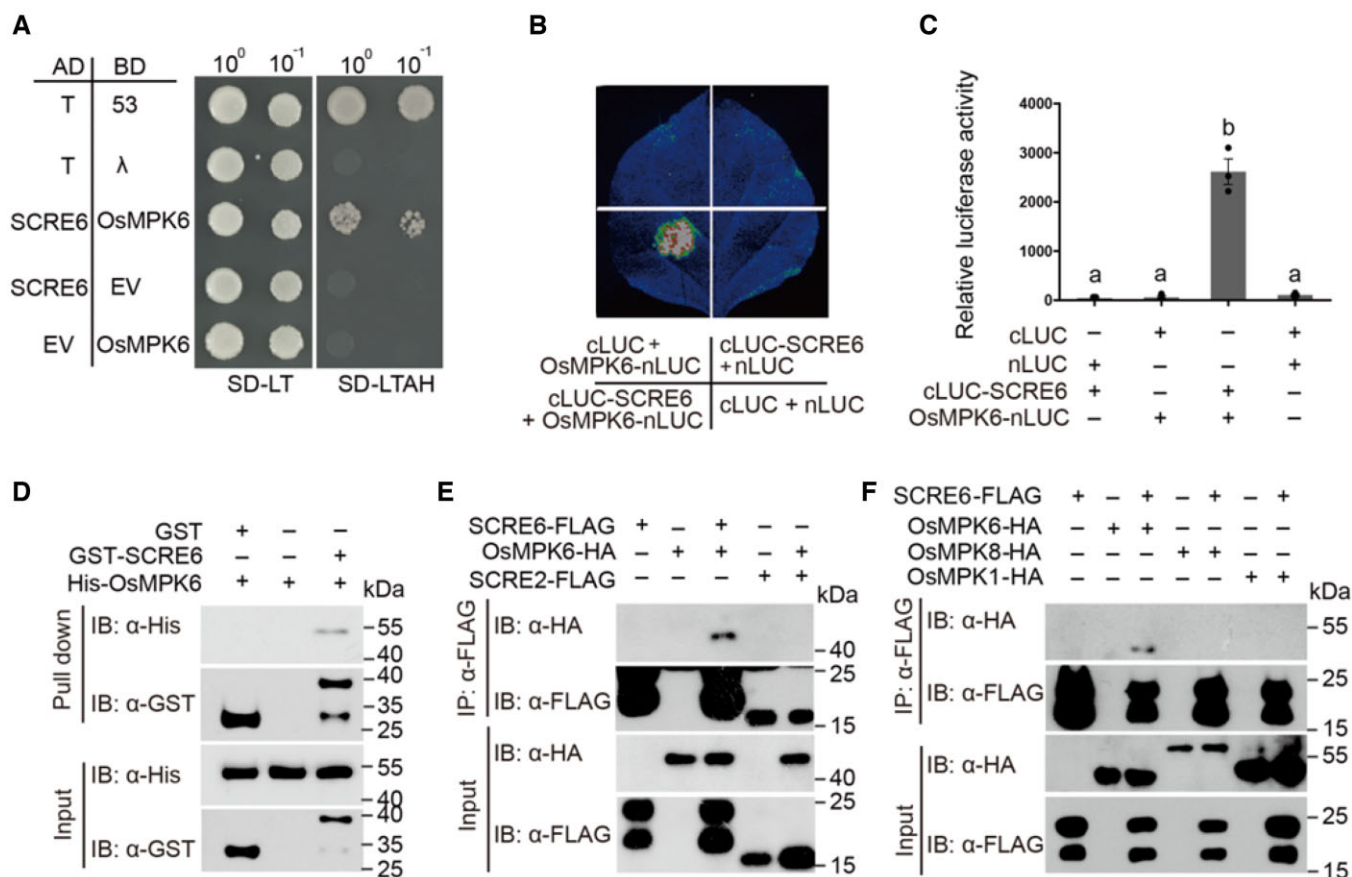
Figure 2 SCRE6 interacts with OsMPK6 in vitro and in vivo. A, The interaction of SCRE6 with OsMPK6 was revealed by yeast two-hybrid assays. The positive interactions were evaluated on media having an SD base lacking Ade, His, Leu, and Trp (SD–LTAH). The pGADT7-T plasmid was transformed with pGBKT7-53 and pGBKT7-λ into yeast cells as the positive and negative controls, respectively. BD, pGBKT7; AD, pGADT7; EV, empty vector. B, Luciferase complementation imaging assay to detect the interaction of SCRE6 with OsMPK6 in *N. benthamiana* leaves. cLUC-SCRE6(−SP) and OsMPK6-nLUC were co-expressed in *N. benthamiana* leaves via *Agrobacterium*-mediated transient expression. The luminescence signal was observed at 48 h after infiltration. C, Quantification of relative luciferase activity in leaves of (B) using a microplate reader. Representative data from three independent assays are shown as mean ± SE ($n = 3$). Different letters (a versus b) indicate significant differences in relative luciferase activity (one-way ANOVA least significant difference test; $P < 0.05$). D, In vitro GST pulldown assay to detect the interaction between SCRE6 and OsMPK6. His-OsMPK6 was pulled down by GST-SCRE6 immobilized on glutathione agarose beads, but not by GST. The input and pulldown proteins were detected with anti-His and anti-GST antibodies. E, F, Co-IP assays used to detect the specific interaction between SCRE6 and OsMPK6 in rice protoplasts. In E, OsMPK6-HA was expressed alone or was co-expressed with SCRE6-FLAG or SCRE2-FLAG in rice protoplasts; in F, OsMPK6-HA, OsMPK1-HA, and OsMPK8-HA were individually co-expressed with SCRE6-FLAG in rice protoplasts. Total protein extracts from transfected protoplasts were incubated with anti-FLAG M2 affinity beads in co-IP assays. The input proteins and precipitants were detected with anti-FLAG and anti-HA antibodies.

The kinase-dead mutant GST-OsMPK6^{KD}, whose conserved Lys72 residue at the ATP binding site was replaced with Arg, was purified and then incubated with GST-OsMKK1^{DD} and ^{32}P-labeled ATP in the presence of GST-SCRE6 or bovine serum albumin (BSA). Autoradiography demonstrated that OsMPK6^{KD} was strongly phosphorylated by OsMKK1^{DD} while the phosphorylation level of OsMPK6^{KD} was significantly reduced in the presence of SCRE6, indicating that SCRE6 decreases OsMKK1^{DD}-mediated OsMPK6^{KD} phosphorylation (Figure 4A). To determine whether SCRE6 attenuates OsMPK6 phosphorylation in vivo, we generated transgenic rice plants that conditionally expressed SCRE6-FLAG as driven by the dexamethasone (DEX) inducible promoter (hereon

called "IE lines"). DEX-induced expression of SCRE6-FLAG was confirmed via immunoblotting (Supplemental Figure S4). Both OsMPK6-FLAG and OsMPK1-FLAG were transiently expressed in rice protoplasts isolated from the transgenic IE-7 seedlings. The transfected rice protoplasts were then treated with DEX or mock solution followed by chitin. OsMPK6-FLAG and OsMPK1-FLAG were immunoprecipitated from protein extracts of transfected protoplasts and then each detected with an anti-p44/42 antibody. OsMPK6 phosphorylation was markedly induced by chitin in the mock-treated IE-7 rice protoplasts, and this chitin-induced phosphorylation was almost completely impeded in the DEX-treated IE-7 rice protoplasts (Figure 4B, left). In contrast, chitin-activated
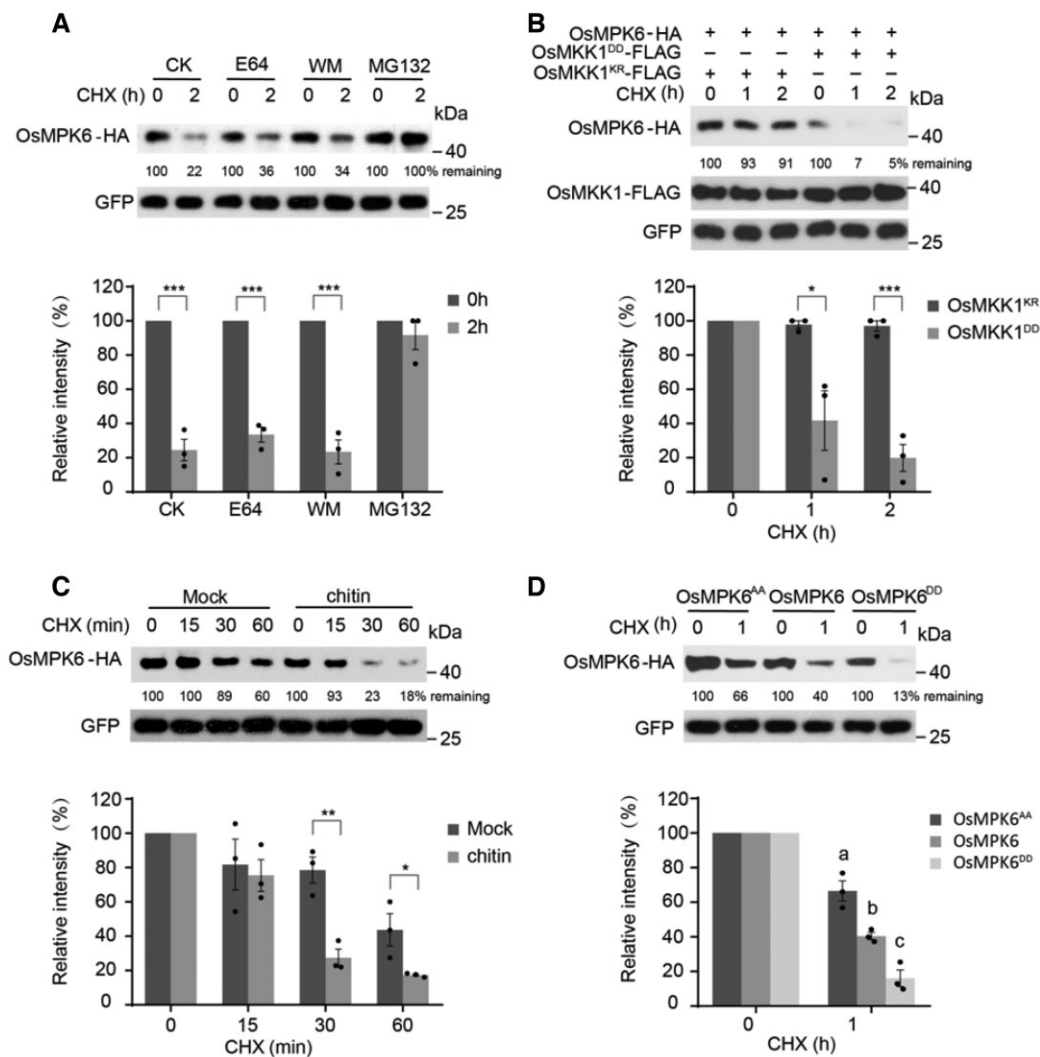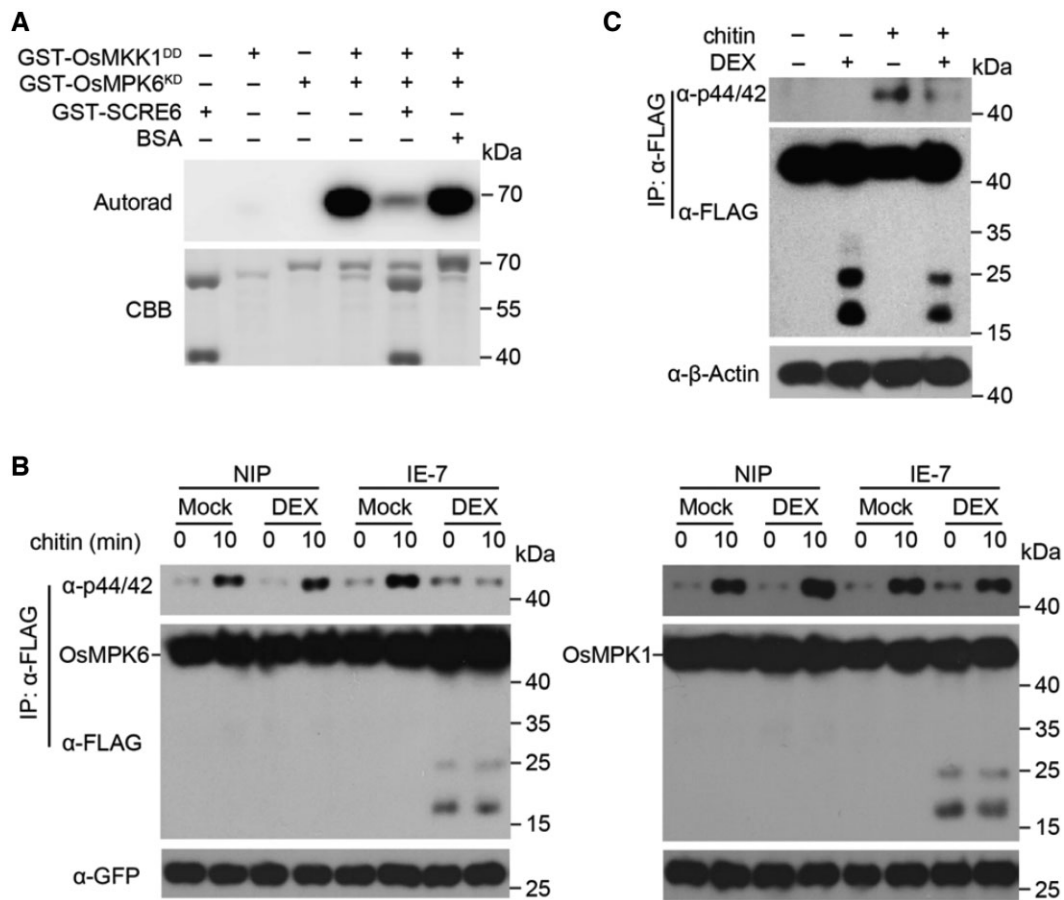
Figure 3 Phosphorylation of OsMPK6 promotes its degradation. A, OsMPK6-HA degradation was detected in the presence of MG132, E64, or WM. OsMPK6-HA was transiently expressed in rice protoplasts. After transfection, rice protoplasts were treated with 50-μM CHX alone or together with MG132 (50 μM), E64 (10 μM), or WM (0.5 μM). OsMPK6-HA abundance was detected by immunoblotting at 0 h and 2 h after the CHX treatment. B, OsMPK6-HA abundance was detected when it was co-expressed with OsMKK1^{DD}-FLAG or OsMKK1^{KR}-FLAG in rice protoplasts. After transfection for 12 h, rice protoplasts were treated with 50-μM CHX for the indicated duration of time. OsMPK6-HA was then detected by immunoblotting with an anti-HA antibody. C, OsMPK6-HA abundance was detected in transfected protoplasts after their treatment with mock or chitin. After undergoing transfection for 12 h, rice protoplasts were treated with 50-μM CHX or 10-μg·mL^{-1} chitin (or mock solution) for the indicated duration of time; OsMPK6-HA was then detected by immunoblotting with an anti-HA antibody. D, The degradation of OsMPK6-HA, OsMPK6^{AA}-HA, and OsMPK6^{DD}-HA was detected in transfected rice protoplasts. After transfection, rice protoplasts were treated with 50-μM CHX and then collected at the indicated time points for immunoblot analyses. In the lower parts of A–D, the band intensities were quantified using ImageJ software. Bars are mean ± SE from three independent experiments. Numbers indicate relative protein levels of OsMPK6-HA normalized to GFP co-expressed in rice protoplasts. In A–C, asterisks indicate significant differences in relative protein levels of OsMPK6 (Student's t test; *** $P < 0.001$, * $P < 0.05$). In D, different letters (a–c) indicate significant differences in relative protein levels of OsMPK6 (one-way ANOVA least significant difference test; $P < 0.05$).

phosphorylation of OsMPK1-FLAG in IE-7 transgenic rice protoplasts was left unaltered by the DEX treatment (Figure 4B, right). In addition, we generated a hybrid of the OsMPK6-FLAG overexpression line and SCRE6-IE transgenic lines by crossing them. Total proteins were extracted from the chitin-treated hybrid seedlings, and then subjected to immunoprecipitation. Immunoblot analysis revealed that chitin-induced phosphorylation of OsMPK6-FLAG was inhibited considerably by the DEX-induced expression of SCRE6-FLAG (Figure 4C).

Altogether, these results indicate that SCRE6 specifically reduces OsMPK6 phosphorylation.

SCRE6 represents a novel family of phosphatases in *U. virens*

To determine how SCRE6 reduces OsMPK6 phosphorylation, we tested whether SCRE6 dephosphorylates OsMPK6. GST-OsMPK6 was first phosphorylated by GST-OsMKK1^{DD} in an in vitro phosphorylation assay;

Figure 4 SCRE6 reduces OsMPK6 phosphorylation in vitro and in vivo. A, Purified GST-SCRE6 decreased the OsMKK1^{DD}-mediated phosphorylation of OsMPK6 as detected by an in vitro kinase assay. In this assay, purified GST-OsMPK6^{KD} and GST-OsMKK1^{DD} were incubated together with GST-SCRE6 or BSA in the presence of ^{32}P-labeled ATP. Top: OsMPK6^{KD} phosphorylation was detected by autoradiography (Autorad). Bottom: Protein loading indicated by CBB staining. B, SCRE6 inhibited the chitin-activated phosphorylation of OsMPK6, but did not affect that of OsMPK1 in rice protoplasts. *OsMPK6-FLAG* (left) and *OsMPK1-FLAG* (right) were transiently expressed in the wild-type (NIP) and IE-7 transgenic rice protoplasts. Transfected rice protoplasts were treated with DEX or a mock solution followed by chitin. Total protein extracts from rice protoplasts were immunoprecipitated with anti-FLAG M2 affinity beads. Top: OsMPK6 and OsMPK1 phosphorylation was detected with an anti-p44/42 antibody. Middle: Protein levels of OsMPK6-FLAG, OsMPK1-FLAG, and SCRE6-FLAG were detected with an anti-FLAG antibody after immunoprecipitation. Bottom: GFP was transiently co-expressed as an internal control. C, Induced expression of *SCRE6-FLAG* attenuated phosphorylation of OsMPK6 in the transgenic hybrid line. Hybrid seedlings (1 week old) of the *OsMPK6-FLAG* overexpression line and *SCRE6-FLAG* IE transgenic line were treated with DEX or a mock solution before receiving a 15-min chitin treatment. Total protein extracts from these treated seedlings were immunoprecipitated with anti-FLAG M2 affinity beads. Top: OsMPK6 phosphorylation was detected with an anti-p44/42 antibody. Middle: Protein levels of OsMPK6-FLAG and SCRE6-FLAG were detected with an anti-FLAG antibody after immunoprecipitation. Bottom: Protein loading is indicated by immunoblotting with anti-β-Actin antibody (α-β-Actin).

after terminating it by adding EDTA, GST-SCRE6, GST-SCRE2 (Fang et al., 2019), or BSA was then added into the reaction mixture (Zhang et al., 2007). Autoradiography uncovered greatly decreased phosphorylation of OsMPK6 after incubation with SCRE6, but it was unchanged following incubation with either SCRE2 or BSA (Figure 5A; Supplemental Figure S5A). These results indicate that SCRE6 functions as a phosphatase or a phospholyase, rather than as a kinase inhibitor. In addition, the phosphorylation level of OsMPK6 was gradually reduced with increasing amounts of SCRE6, indicating that SCRE6 dephosphorylates OsMPK6 in a dose-dependent way (Supplemental Figure S5A).

To rule out the possibility that SCRE6 has a phospholyase activity, pre-phosphorylated His-OsMPK6 by GST-OsMKK1^{DD} was first dephosphorylated by GST-SCRE6 and by calf intestine alkaline phosphatase (CIAP). After removing the GST-tagged proteins with GST beads, His-OsMPK6 was enriched using a nickel column and then incubated with GST-OsMKK1^{DD} in the phosphorylation assay. Immunoblotting with an anti-p44/42 antibody revealed that OsMPK6 dephosphorylated by SCRE6 and CIAP was capable of being re-phosphorylated, indicating that SCRE6-mediated dephosphorylation is reversible (Supplemental Figure S5B). Furthermore, we conducted an in vitro phosphatase assay where GST-SCRE6 was incubated with the chromogenic substrate
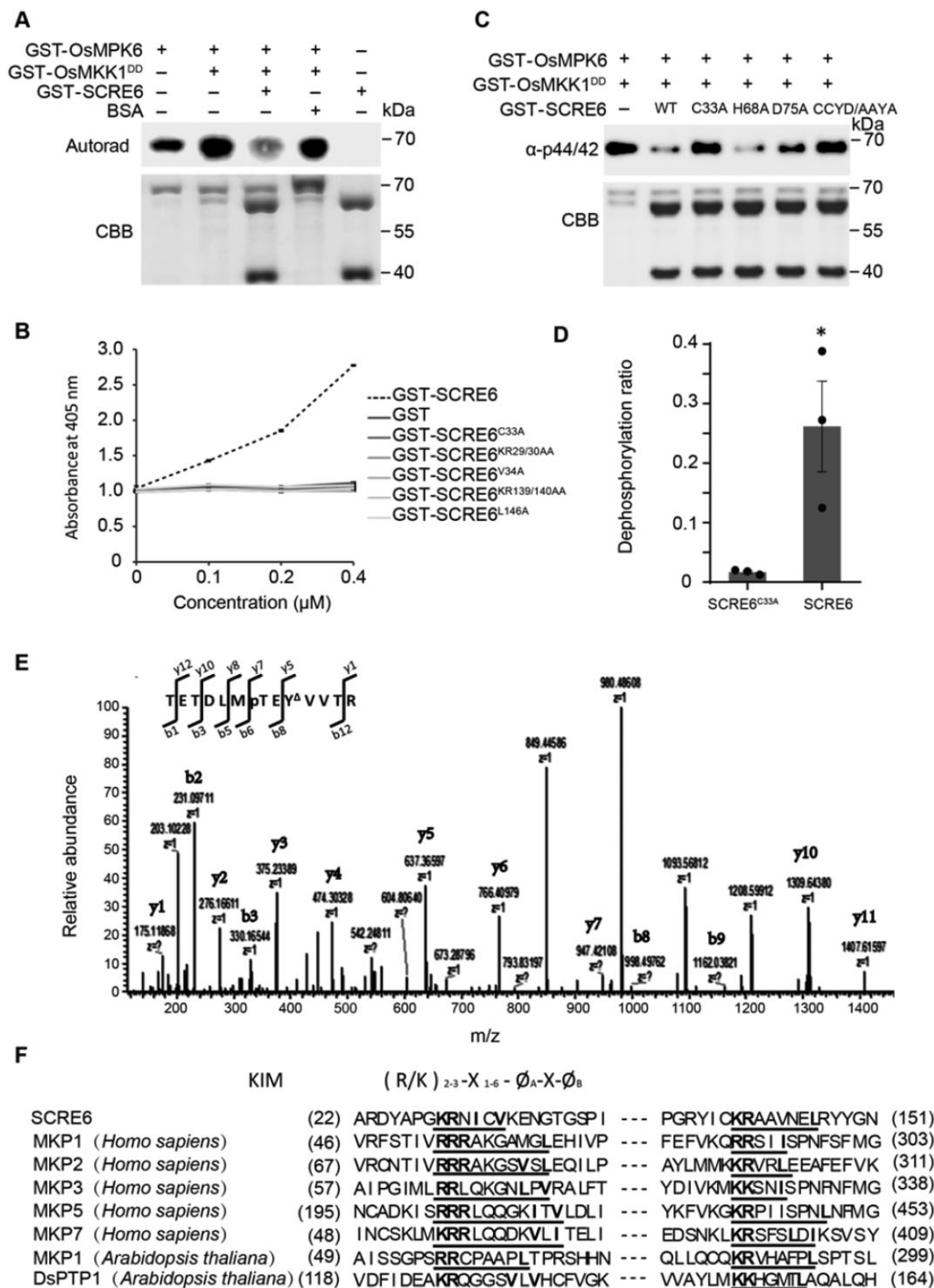
Figure 5 SCRE6 is a tyrosine phosphatase and dephosphorylates OsMPK6 in vivo and in vitro. A, SCRE6 dephosphorylated OsMPK6 in vitro. Purified GST-OsMPK6 was incubated with GST-OsMKK1^{DD} in the presence of ^{32}P-labeled ATP in an in vitro kinase assay. The reaction was terminated by adding 10-mM EDTA followed by incubation with purified GST-SCRE6 or BSA. Top: OsMPK6 phosphorylation was detected by autoradiography (Autorad) after a 30-min incubation. Bottom: Protein loading is indicated by CBB staining. B, In vitro phosphatase assay to detect the phosphatase activity of SCRE6 and its variants. In this assay, different concentrations of GST-SCRE6, its variants or GST were incubated with *p*-NPP. The yellow product *p*-nitrophenol was evaluated based on the absorbance at 405 nm. C, The ability of different SCRE6 variants to dephosphorylate OsMPK6 was detected in an in vitro dephosphorylation assay. Phosphorylated GST-OsMPK6 by GST-OsMKK1^{DD} was incubated with GST-SCRE6, SCRE6^{C33A}, SCRE6^{H68A}, SCRE6^{D75A} or SCRE6$^{CCYD/AAYA}$ for 30 min. Top: The phosphorylation level of OsMPK6 was detected with anti-p44/42 antibodies. Bottom: Protein loading is indicated by CBB staining. D, Quantification of the TETDLMpTEpYVVTR phosphopeptide dephosphorylated by SCRE6 and SCRE6^{C33A}. Dephosphorylated peptides were detected by liquid chromatography tandem mass spectrometry and the PRM method. Peptide dephosphorylation ratios (dephosphorylated/phosphorylated peptides) were determined using Xcalibur software. A significant difference between treatments is indicated by asterisks (Student's *t* test; *$P < 0.05$). E, Phosphotyrosine, but not phosphothreonine, in the

(continued)

p-nitrophenylphosphate (p-NPP). The expected yellow product p-nitrophenol was generated and detectable from this assay, confirming that SCRE6 possessed phosphatase activity (Figure 5B). To further verify the specificity of SCRE6 dephosphorylating OsMPK6, through an in vitro dephosphorylation assay, we showed that phosphorylation of OsMPK1 mediated by OsMKK5^{DD} was not altered by SCRE6 (Supplemental Figure S5C). The results indicate that SCRE6 dephosphorylates OsMPK6 specifically.

In most cases, the conserved Cys residue is the enzymatically active site for Tyr protein phosphatases and likewise the conserved Asp or His residue for Ser/Thr protein phosphatases (Shi, 2009; Tonks, 2013). To identify the key residue(s) responsible for phosphatase activity of SCRE6, a total of 12 SCRE6 variants whose Cys, Asp, and His residues except for Asp24 were replaced individually with Ala were generated and then purified for phosphatase assays. Mutations in the conserved Cys33 residue at the N-terminal domain (SCRE6^{C33A}) and in the Asp75 residue at the conserved CCXD motif (SCRE6^{D75A}) caused a reduction in phosphatase activity (Figure 5C). Further, these two SCRE6 variants interacted with OsMPK6, as detected by the yeast two-hybrid assay (Supplemental Figure S5D). In contrast, other SCRE6 variants with single-point mutations retained their ability to dephosphorylate OsMPK6 (Figure 5C; Supplemental Figure S5E).

To determine which family of phosphatases SCRE6 actually belongs to, a synthetic 13-amino-acid phosphopeptide (TETDLMpTEpYVVTR) containing phosphothreonine (pT201) and phosphotyrosine (pY203), derived from the TEY motif of OsMPK6, was incubated with SCRE6 and SCRE6^{C33A}. The products were subject to mass spectrogram analysis that used parallel reaction monitoring (PRM) after removing SCRE6 via ultrafiltration. Dephosphorylation of the synthetic phosphopeptide was quantified using Xcalibur software. The ratio of dephosphorylated/phosphorylated phosphopeptide was significantly greater after the SCRE6 co-incubation than the SCRE6^{C33A} co-incubation (Figure 5D). Fragmentation of the phosphopeptide was analyzed by tandem mass spectrometry. The phosphotyrosine (pY203), but not pT201, was identified as the dephosphorylation site due to the loss of a phosphate group (80 Da). The results suggest that SCRE6 functions as a tyrosine phosphatase (Figure 5E).

Through PSI-BLAST searches, no SCRE6 homolog could be identified from other fungal species, while three putative *U. virens* effectors, namely UV_4984, UV_2239, and UV_642, were found to be homologous with SCRE6 (Supplemental Figure S6A). Yeast two-hybrid assays demonstrated that

these SCRE6 homologs also interacted with OsMPK6 (Supplemental Figure S6B). In vitro dephosphorylation assays showed that the SCRE6 homologs were all capable of dephosphorylating OsMPK6 (Supplemental Figure S6C). Consistently, in vitro phosphatase assays revealed that the homologs of SCRE6 possessed phosphatase activity, although the magnitude of their enzyme activity was significantly less than that of SCRE6 (Supplemental Figure S6D). Next, gene expression analyses uncovered the expression levels of *SCRE6* homologous genes, which were barely or only slightly upregulated during *U. virens* infection, in stark contrast to *SCRE6* expression, which was highly upregulated after infection (Figure 1C; Supplemental Figure S6E). Collectively, we concluded that SCRE6 and its homologs were able to dephosphorylate OsMPK6 and constituted a MAPK phosphatase family.

Interestingly, multi-sequence alignment among the SCRE6 homologs identified a conserved basic and hydrophobic motif at the N-termini of these homologs (Supplemental Figure S6A). Through PSI-BLAST searches against the conserved motif, we found that the conserved basic and hydrophobic motifs at the N- and C-termini of SCRE6 are highly similar to the kinase interaction motifs (KIMs) in the MAPK phosphatase family in both *Homo sapiens* and *Arabidopsis thaliana* (Figure 5F; Liu et al., 2006; Bartels et al., 2010). To investigate the necessity of these KIMs for SCRE6 functioning, we generated several SCRE6 variants: SCRE6$^{KR29/30AA}$, SCRE6^{V34A}, SCRE6$^{KR139/140AA}$ and SCRE6^{L146A}. These variants completely lost their phosphatase activity, substantiating the indispensability of these conserved basic and hydrophobic amino-acid residues for SCRE6's phosphatase activity (Figure 5B). However, no canonical catalytic motif "HCXXXXXR", a characteristic of protein tyrosine phosphatases (PTPs) and dual-specificity phosphatases, was identified in SCRE6 (Keyse, 2000). Together, our experimental data and bioinformatics analysis strongly indicate that SCRE6 is a fungal MAPK tyrosine phosphatase that lacks the canonical phosphatase motif.

SCRE6 specifically enhances the stability of OsMPK6 in vivo

Based on the above findings, we speculated that SCRE6 ectopically expressed in rice could stabilize OsMPK6 by functioning as a MAPK phosphatase to dephosphorylate the protein. We demonstrated that the abundance of OsMPK6 was much higher in the DEX-treated IE-7 transgenic line than that in either the wild-type or mock-treated IE-7 transgenic plants, indicating that SCRE6 promotes the accumulation of OsMPK6 (Figure 6A). In addition, reverse

Figure 5 (Continued)
phosphopeptide was dephosphorylated by SCRE6. The SCRE6-treated phosphopeptide was analyzed by tandem mass spectrometry. The fragmentation profile is indicated by the b and y ions. The amino acid sequence of the peptide is shown at the top-left, and Y$^{\Delta}$ marks the SCRE6-modified phosphotyrosine residue. F, Multisequence alignment for SCRE6 and dual-specificity phosphatases from the MKP family in *H. sapiens* and Arabidopsis. The KIMs are underlined. Basic residues (R/K) and hydrophobic residues (Ø$_A$ and Ø$_B$) are marked in bold. Numbers in parentheses indicate the amino acid number.
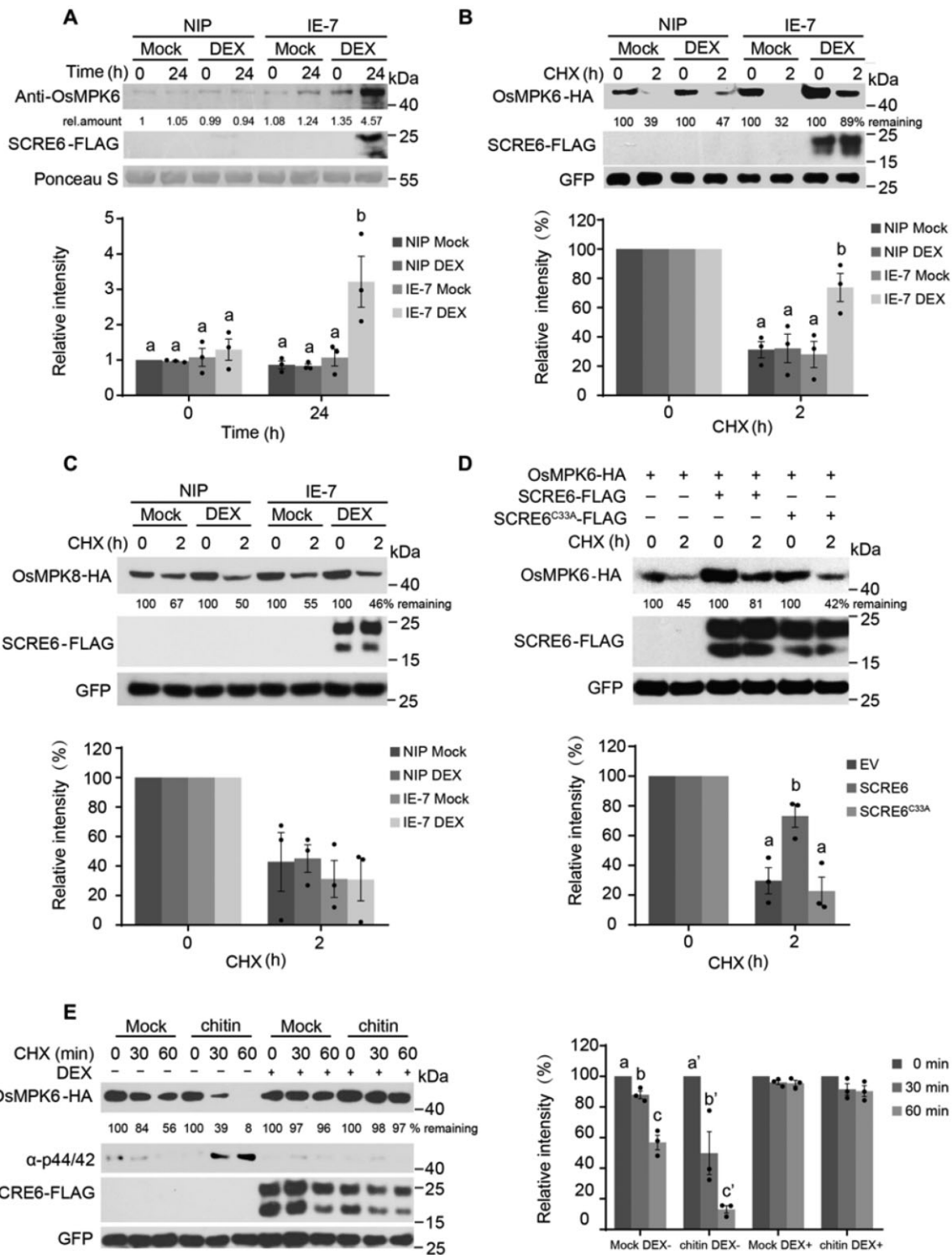
Figure 6 SCRE6 stabilizes OsMPK6 in rice. A, Endogenous protein levels of OsMPK6 in the wild-type and IE-7 transgenic seedlings. One-week-old seedlings were treated with DEX or a mock solution for 24 h before protein extractions. Top: Total protein extracts were detected by immunoblotting with anti-OsMPK6 and anti-FLAG antibodies. Bottom: Protein loading is indicated by Ponceau S staining. Numbers indicate arbitrary relative units of OsMPK6-HA calculated from the densitometry measurements. B, C, Protein levels of OsMPK6-HA (B) and OsMPK8-HA (C) transiently expressed in the mock- and DEX-treated wild-type and IE-7 transgenic rice protoplasts. Transfected rice protoplasts were treated for 2 h with the protein synthesis inhibitor CHX (50 µM). Protein abundance was detected via immunoblotting with the indicated antibodies. GFP was transiently co-expressed as an internal control. Numbers indicate relative protein levels normalized to GFP. D, Protein degradation assay used to detect the ability of SCRE6^{C33A} to stabilize OsMPK6 in rice protoplasts. OsMPK6-HA was co-expressed with *SCRE6-FLAG* or *SCRE6^{C33A}-FLAG* in rice protoplasts. The transfected protoplasts were treated with CHX (50 µM). The abundance of OsMPK6-HA was detected by immunoblotting

(continued)

transcription quantitative polymerase chain reaction (RT-qPCR) revealed that the transcript level of *OsMPK6* was not significantly altered by the DEX treatment in the *SCRE6* IE transgenic lines (Supplemental Figure S7A); this suggests that SCRE6 does not transcriptionally regulate *OsMPK6* expression. Next, we performed a protein degradation assay in rice protoplasts. The protoplasts isolated from the wild-type and IE-7 transgenic seedlings were incubated with DEX or a mock solution during the pUC19-*OsMPK6-HA* transfection; GFP was co-expressed in rice protoplasts as an internal control. After transfection, the protoplasts were treated with CHX to inhibit protein synthesis. Immunoblot analyses showed that the abundance of OsMPK6-HA in the DEX-treated IE-7 protoplasts surpassed that in the wild-type and mock-treated IE-7 protoplasts after CHX treatment (Figure 6B). Furthermore, we demonstrated that transiently expressed OsMPK8-HA was rapidly degraded in rice protoplasts after undergoing the CHX treatment, whereas the degradation rate of OsMPK8-HA in the DEX-treated IE-7 transgenic line was similar to that in the wild-type and mock-treated IE-7 transgenic cells (Figure 6C). These findings indicate that SCRE6 inhibits the degradation of OsMPK6 but does not alter the stability of OsMPK8. We then showed that the abundance of OsMPK6 was much lower when it was co-expressed with SCRE6^{C33A} in rice protoplasts compared with its co-expression with SCRE6 (Figure 6D). These data indicate that the C33A mutation robs SCRE6 of its ability to stabilize OsMPK6 and that SCRE6 stabilizes OsMPK6 through dephosphorylation. Interestingly, chitin-promoted OsMPK6 degradation and phosphorylation were also significantly inhibited in the IE-7 transgenic line after the DEX treatment, suggesting that SCRE6 expression inhibits chitin-enhanced degradation of OsMPK6 (Figure 6E). Taken together, these results indicate that SCRE6 enhances the stability of OsMPK6 in particular.

The overexpression of OsMPK6 activates SA and JA signaling in rice (Shen et al., 2010). Therefore, we speculated that DEX-induced expression of SCRE6 in the IE transgenic lines enhances JA and SA signaling. To test this hypothesis, we performed RT-qPCR assays, finding that the JA-responsive genes *LOX2*, *AOS2*, and *JAMyb*, as well as the SA-responsive gene *WRKY45*, were all significantly upregulated in the DEX-treated IE-7 transgenic line in comparison with the wild-type and mock-treated transgenic plants (Supplemental Figure S7, B–E) substantiates our speculation.

Ectopic expression of *SCRE6* suppresses plant immunity and promotes disease susceptibility in rice

OsMPK6 is a crucial negative regulator of plant immunity to *Xoo* (Wang et al., 2021a). We investigated whether OsMPK6 is involved in plant resistance to *U. virens*. The wild-type and *OsMPK6*-overexpressing transgenic lines were injection-inoculated with *U. virens*. Significantly more false smut balls formed on the inoculated panicles of OsMPK6-overexpressing transgenic lines than on those of the wild-type plants (Supplemental Figure S8). Given that SCRE6 stabilizes the negative immune regulator OsMPK6, we next determined whether SCRE6 could inhibit PAMP-induced immune responses in the transgenic plants. These results showed that chitin-induced MAPK activation was attenuated in the *SCRE6*-expressing transgenic lines vis-à-vis the wild type (Figure 7A). Besides, expression of *OsPR5* and *OsPR10a* induced by chitin was significantly suppressed in the DEX-treated IE transgenic lines in comparison with the wild-type and mock-treated IE transgenic plants (Figure 7, B and C). Subsequently, the wild-type, IE-7, and IE-41 transgenic lines were injection-inoculated with *U. virens*. False smut balls formed on the inoculated panicles of the DEX-treated IE-7 and IE-41 transgenic lines were more abundant than those formed on the panicles of the wild-type and mock-treated transgenic plants (Figure 7D; Supplemental Figure S9A). Furthermore, the wild-type and IE transgenic lines were challenged with the bacterial blight pathogen *X. oryzae* pv. *oryzae* PXO99 after undergoing the DEX and mock treatments. The inoculated leaves in the DEX-treated IE-7, IE-41, and IE-55 transgenic plants exhibited significantly longer disease lesions than those of the wild-type and mock-treated transgenic plants (Supplemental Figure S9, B and C). Together, the results demonstrated that the induced expression of SCRE6 in rice caused its greater susceptibility to false smut and bacterial blight diseases.

Phosphatase activity of SCRE6 is essential for its virulence function

To clarify whether phosphatase activity is required for the virulence function of SCRE6, we tried to complement the Δ*scre6*-39 mutant by expressing the SCRE6^{C33A} mutant protein. Inoculation assays demonstrated that the *SCRE6*^{C33A} complementation strain did not restore the *U. virens* virulence to rice, whereas the *SCRE6* complementation strain largely did (Figure 8A; Supplemental Figure S10A).
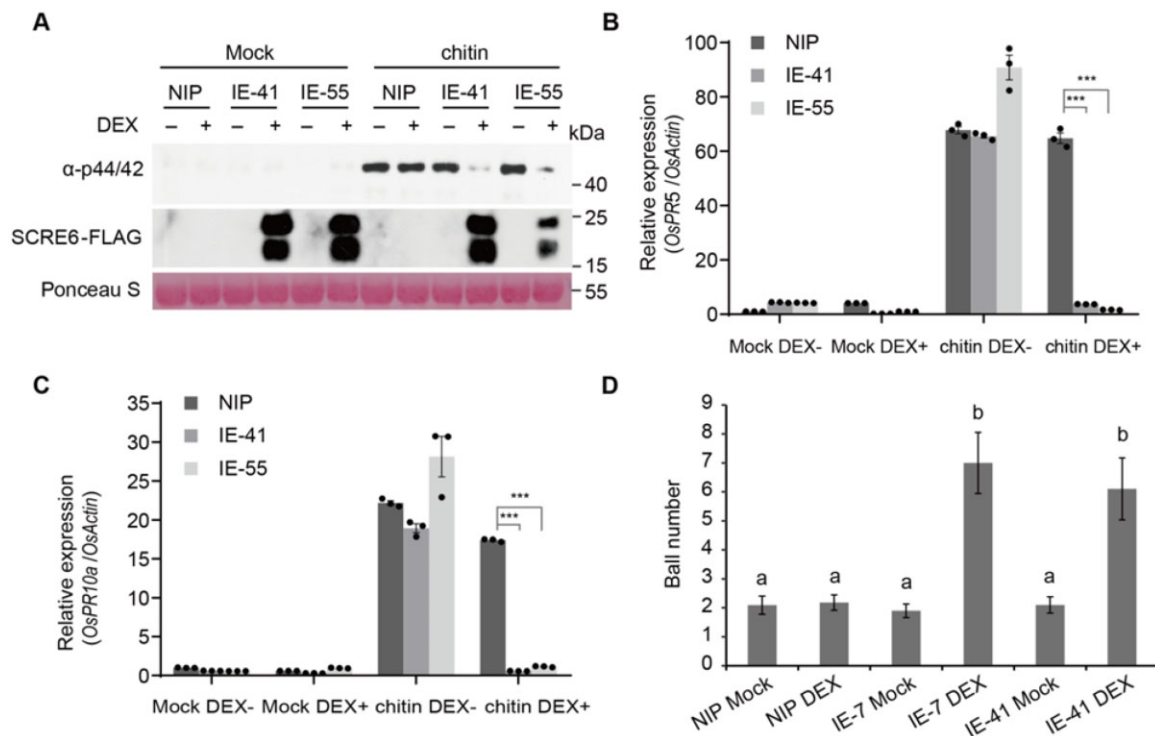
Figure 6 (Continued)
at 0 h and 2 h after the CHX treatment. GFP was transiently co-expressed as an internal control. E, OsMPK6-HA protein levels in the mock- and DEX-treated IE-7 transgenic rice protoplasts in response to the mock and chitin treatments. After transfection for 12 h, rice protoplasts were incubated with 50-μM CHX and 10-μg·mL^{-1} chitin (or mock solution) for the indicated duration of time. Bottom: GFP was transiently co-expressed as an internal control. In the lower parts of A–D and in the right part of E, band intensities were quantified by densitometry using ImageJ software. Bars are mean ± SE from three independent experiments. Numbers indicate relative protein levels normalized to GFP. Different letters (a–c′) indicate significant differences in protein levels between different treatments (one-way ANOVA LSD test; $P < 0.05$).

Figure 7 Ectopic expression of *SCRE6* inhibits PAMP-triggered immunity and causes enhanced disease susceptibility to false smut in rice. A, Chitin-induced MAPK activation was attenuated in the *SCRE6*-expressing IE transgenic lines. One-week-old seedlings were treated with DEX or mock solution for 16 h before the chitin treatment. MAPK activation and SCRE6-FLAG expression were detected by immunoblotting with anti-p44/42 and anti-FLAG antibodies, respectively. Protein loading is indicated by Ponceau S staining. B and C, Chitin-induced expression of *OsPR5* (B) and *OsPR10a* (C) was significantly inhibited in DEX-treated IE transgenic lines vis-à-vis the wild-type seedlings. One-week-old seedlings were treated with DEX or mock solution for 16 h before receiving the chitin treatment. Expression levels of the defense marker genes *OsPR5* and *OsPR10a* were detected by RT-qPCR. *OsActin* served as an internal control. Bars are the mean ± SE (*n* = 3). Asterisks indicate significant differences in the expression levels of *PR* genes between the wild-type and DEX-treated IE transgenic lines (Student's *t* test; ***$P < 0.001$). D, Disease severity on rice panicles of the wild-type (NIP), IE-7 and IE-41 transgenic plants after their inoculation with *U. virens*. Young rice panicles were injection-inoculated with the virulent isolate JS60-2 after undergoing a mock or DEX treatment. False smut balls formed on rice panicles of the wild-type and IE-7 and IE-41 transgenic lines were counted at 1 month after *U. virens* inoculation. Bars are the mean ± SE (*n* = 11, 11, 10, 10, 10, and 10, respectively). Different letters (a and b) indicate significant differences in the number of smut balls formed on the inoculated panicles of IE-7 and IE-41 transgenic plants after undergoing the mock and DEX treatments (one-way ANOVA least significant difference test; $P < 0.05$).

Furthermore, we generated transgenic rice lines that had DEX-induced expression of *SCRE6*[C33A] (called IE-C33A lines hereinafter). Evidently, chitin-induced MAPK activation was not altered in the DEX-treated IE-C33A transgenic line when compared with the wild-type plants (Figure 8B). Consistently, the chitin-induced expression of *OsPR5* and *OsPR10a* in the DEX-treated IE-C33A transgenic line did not differ from that in the wild-type plants (Figure 8, C and D). The wild-type and IE transgenic seedlings (IE-7, IE-41, and IE-C33A) were also challenged with the *M. oryzae* isolate SZ4 after the DEX and mock treatments. DEX-induced expression of SCRE6 in IE-7 and IE-41 transgenic lines enhanced disease symptoms and fungal biomass caused by *M. oryzae*, whereas DEX-induced expression of SCRE6[C33A] in the IE-C33A transgenic line did not alter disease severity relative to the wild-type and mock-treated transgenic lines (Supplemental Figure S10B). Altogether these results indicate that the Cys33 residue in SCRE6 is essential for its virulence function.

Discussion

Ustilaginoidea virens secretes a large arsenal of effectors to promote its infection of host plants (Sun et al., 2020). Elucidating the molecular mechanisms underlying virulence functions of *U. virens* effectors is especially valuable for developing a sound disease management strategy (Sun et al., 2020). In this study, we identified SCRE6 as an important virulence effector in *U. virens*. SCRE6 and its homologs represent a family of MAPK phosphatases that dephosphorylate and stabilize OsMPK6 in rice plants.

In our earlier study, SCRE6 was shown to suppress HR in *N. benthamiana* (Zhang et al., 2014). Here, we demonstrated that *SCRE6* is required for *U. virens* virulence to rice (Figure 1A). In addition, SCRE6 has typical features characteristic of a fungal effector protein: it is a secreted protein and is transcriptionally induced during infection (Figure 1, B and C). By virtue of the secretion system of *M. oryzae*, ectopically expressed SCRE6 in *M. oryzae* was proven to accumulate in the BIC, through which SCRE6 is translocated into
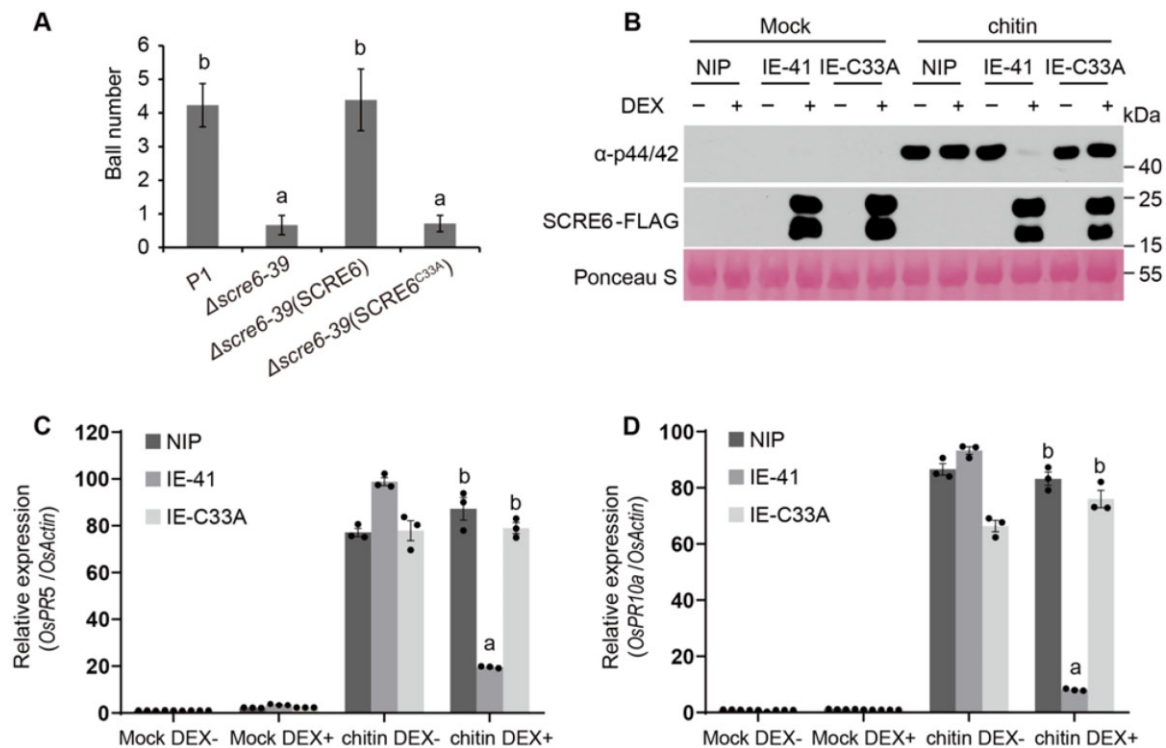
Figure 8 Phosphatase activity of SCRE6 is essential for its virulence function. A, The complementation strain expressing SCRE6^{C33A} lost the ability to restore the virulence of *U. virens*. The wild-type, Δ*scre6*-39, and complementation strains Δ*scre6*-39 (SCRE6) and Δ*scre6*-39 (SCRE6^{C33A}) were injected into young panicles of the rice cultivar LYP9. False smut balls were counted about 1 month post-inoculation. Bars are the mean ± SE (n = 13, 14, 13, and 14, respectively). Different letters (a and b) indicate significant differences in the number of false smut balls formed after inoculation with the wild-type, Δ*scre6*-39, and complementation strains (one-way ANOVA least significant difference (LSD) test; $P < 0.05$). B, Phosphorylation levels of MAPK in the wild-type, SCRE6-, and SCRE6^{C33A}-expressing transgenic IE lines after undergoing the mock and chitin treatments. One-week-old seedlings were treated with DEX or a mock solution for 16 h before the mock and chitin treatments. MAPK activation and SCRE6-FLAG expression were detected by immunoblotting with anti-p44/42 and anti-FLAG antibodies, respectively. Protein loading is indicated by Ponceau S staining. C and D, Expression levels of *OsPR5* (C) and *OsPR10a* (D) in the wild-type, SCRE6-, and SCRE6^{C33A}-expressing IE transgenic lines after the mock and chitin treatments. One-week-old seedlings were treated with DEX or mock solution for 16 h before receiving the mock and chitin treatments. Expression levels of the defense marker genes *OsPR5* and *OsPR10a* were detected by RT-qPCR. *OsActin* served as an internal control. Bars are the mean ± SE (n = 3). Different letters (a and b) indicate significant differences in the expression level of *PR* genes between the wild-type and IE-41 transgenic lines (one-way ANOVA LSD test; $P < 0.05$).

rice cells (Khang et al., 2010; Figure 1, D and E). Through the observation of protein translocation via BIC in *M. oryzae*, we learned that multiple secreted proteins in *M. oryzae* and *U. virens* are cytoplasmic effectors that are translocated into host cells through the BIC, a specialized secretion structure (Khang et al., 2010; Zhang et al., 2020). Taken together, we conclude that SCRE6 is a key effector protein that contributes to *U. virens* virulence to rice.

Multiple approaches including luciferase complementation imaging, co-IP, and GST pull-down assays identified OsMPK6 as a target of SCRE6 in rice (Figure 2). OsMPK6 is a crucial MAPK that negatively regulates plant immunity through a phosphorelay system (Wang et al., 2021a). In plant defense signaling, phosphorylation alters protein function and stability (Mithoe and Menke, 2018). After the receptor-like cytoplasmic kinase PBL13 phosphorylates the conserved Ser862 and Thr912 residues at the C-terminus of the plant NADPH oxidase RBOHD, the RING-finger E3 ligase PIRE enhances the ubiquitination of RBOHD, resulting in

less RBOHD abundance and reduced ROS production (Lee et al., 2020). In Arabidopsis, the abundance of BIK1, a critical regulator of plant immunity, is positively regulated by its phosphorylation. Unphosphorylated BIK1 is more prone to be ubiquitinated by PUB25 and PUB26 for its degradation, whereas activated BIK1 is more stable in Arabidopsis (Wang et al., 2018). In contrast to that, we demonstrated that both the phosphomimetic mutation and PAMP-induced phosphorylation of OsMPK6 promoted its degradation significantly (Figure 3). Similarly, flg22 treatment promotes the degradation of calcium-dependent protein kinase CPK28 in Arabidopsis. The association between CPK28 and the E3 ligases ATL31/6 is enhanced after flg22 treatment and thereby enhances CPK28 ubiquitination and degradation (Liu et al., 2022). It will be interesting to investigate the OsMPK6 degradation mechanism and to explain how OsMPK6 phosphorylation promotes its degradation.

The above findings spurred us to investigate whether SCRE6 alters OsMPK6 phosphorylation. We revealed that

SCRE6 inhibited the in vitro and in vivo phosphorylation of OsMPK6 (Figure 4). The type III secreted effector HopPtoD2/HopAO1 in *P. syringae* pv. *tomato* has been reported to be a tyrosine phosphatase (Espinosa et al., 2003; Macho et al., 2014; Luo et al., 2020). In addition, another effector HopAI1 in *P. syringae* functions as a phosphothreonine lyase mediating irreversible dephosphorylation (Zhang et al., 2007). Therefore, we speculate that SCRE6 decreases the phosphorylation level of OsMPK6 through three possible mechanisms: inhibiting OsMKK1 kinase activity, blocking OsMPK6 phosphorylation, and functioning as a phosphatase or phospholyase to dephosphorylate OsMPK6. To determine how SCRE6 reduces OsMPK6 phosphorylation, we first performed a comprehensive bioinformatic analysis to predict the structural features and functional domains of the effector by conducting HHpred, PSI-BLAST, and SMART domain searches, but we failed to identify any known domains (Altschul et al., 1997; Soding et al., 2005; Letunic and Bork, 2018). Nevertheless, the subsequent experiments confirmed that SCRE6 is a tyrosine phosphatase. First, the in vitro dephosphorylation assay showed that pre-phosphorylated OsMPK6 by OsMKK1 was dephosphorylated by SCRE6 (Figure 5A). Moreover, an in vitro phosphatase assay using the chromogenic *p*-NPP as a substrate confirmed that SCRE6 had phosphatase activity (Figure 5B). Thirdly, a synthetic phosphopeptide carrying *p*-threonine and *p*-tyrosine derived from the TEY motif in OsMPK6 was dephosphorylated by SCRE6, but not by SCRE6^{C33A} (Figure 5D). Furthermore, the finding that SCRE6-mediated dephosphorylation is reversible rules out the possibility of SCRE6 functioning as a phopholyase (Supplemental Figure S5B). Mass spectrogram analysis revealed that the phosphate group was removed from phosphotyrosine rather than from phosphothreonine in the synthetic phosphopeptide by SCRE6, offering compelling evidence that SCRE6 is a tyrosine phosphatase (Figure 5E). Overall, we conclude that SCRE6 serves as a tyrosine phosphatase to dephosphorylate OsMPK6.

Through PSI-BLAST searches, we identified three SCRE6 homologs in *U. virens*: the putative effectors UV_4984, UV_2239, and UV_642 (Supplemental Figure S6A). These SCRE6 homologs all interacted with and dephosphorylated OsMPK6, although they have a much lower phosphatase activity than does SCRE6 (Supplemental Figure S6, B–D). In addition, the expression of *SCRE6* homologous genes is negligibly induced during *U. virens* infection (Supplemental Figure S6E). These findings could explain why the Δ*scre6* single knockout mutant incurred a significant reduction in virulence to rice. Interestingly, a conserved basic and hydrophobic region, which is characteristic of the KIMs in MAPK phosphatases, was identified from the N-termini of these homologs (Supplemental Figure S6A). Based on this finding, we conducted a sequence alignment of SCRE6 and MAPK phosphatases in *H. sapiens* and Arabidopsis; this revealed that SCRE6 harbors two KIMs at its N- and C-terminal domains, respectively (Figure 5F; Liu et al., 2006;

Bartels et al., 2010). These basic and hydrophobic residues are required for the phosphatase activity of SCRE6 (Figure 5B). Protein tyrosine phosphatases (PTPs), serine–threonine phosphatases (STPs), or dual-specificity (Ser/Thr and Tyr) phosphatases (DSPs) have been demonstrated to inactivate MAPKs in multiple model organisms (Bartels et al., 2010). Most of the PTP and DSPs targeting MAPKs contain an essential cysteine residue for the enzymatic activity at the conserved catalytic signature $C(X)_5R$ (Kerk et al., 2008). However, SCRE6 contains no such conserved $C(X)_5R$ motif. Through alanine scanning mutagenesis, we show that mutations of the conserved Cys33 and Asp75 residues at the CCXD motif cause SCRE6 to lose much of its phosphatase activity (Figure 5C; Supplemental Figure S5E). However, further investigations are needed to identify the catalytic active motif in SCRE6. In summary, SCRE6 may represent the prototype of a family of tyrosine MAPK phosphatases lacking the canonical catalytic motif.

OsMPK6 degradation is promoted by its phosphorylation, which is mitigated by SCRE6. Consistently, the OsMPK6 stability assays in *SCRE6*-expressing rice protoplasts and transgenic plants showed that OsMPK6 abundance was significantly greater in *SCRE6*-expressing transgenic plants than in the wild type (Figure 6A). In contrast, the transcript level of *OsMPK6* was unaltered by the induced expression of SCRE6 in transgenic plants (Supplemental Figure S7A). Several pathogen effectors have been reported to alter host protein stability and regulate plant immunity through different molecular strategies (Tariqjaveed et al., 2021). The *U. maydis* effector Tin2 masks a ubiquitin–proteasome degradation motif in ZmTTK1, a protein kinase in maize (*Zea mays*), to stabilize the active kinase (Tanaka et al., 2014). The cytoplasmic effector OSP24 in *Fusarium graminearum* competes against an orphan protein TaFROG for binding with TaSnRK1α to accelerate the degradation of TaSnRK1α via the ubiquitin-26S proteasome in wheat (*Triticum aestivum*; Jiang et al., 2020). More recently, the novel type III effector kinase XopC2 has been identified to specifically phosphorylate the Ser53 residue in OSK1 and facilitate the formation of the SCF^{OsCOI1b} complex that promotes the degradation of JAZ proteins (Wang et al., 2021b). Here, we demonstrated that SCRE6 serves as a phosphatase to dephosphorylate OsMPK6 and inhibits the degradation of OsMPK6. The supporting experimental data include that OsMPK6-HA degradation was significantly and specifically inhibited by SCRE6 but not by SCRE6^{C33A} in transfected protoplasts (Figure 6, B and D). Besides, the expression levels of *LOX2*, *AOS2*, *JAMyb*, and *WRKY45* were significantly enhanced in *SCRE6*-expressing transgenic plants (Supplemental Figure S7, B–E). This finding is consistent with a previous report showing that the JA- and SA-responsive genes are transcriptionally upregulated in *OsMPK6*-overexpressing transgenic lines (Shen et al., 2010). Importantly, SCRE6 does not influence the stability of OsMPK8 (Figure 6C). Therefore, SCRE6 specifically prevents OsMPK6 degradation in rice.

We demonstrated that immune responses, including PAMP-induced *PR* gene expression and MAPK activation, were significantly inhibited in these *SCRE6*-expressing transgenic rice plants, but they were not suppressed in the *SCRE6*^{C33A}-expressing plants (Figures 7, A–C and 8, B–D). Ectopic expression of SCRE6 in the transgenic rice plants caused an enhanced susceptibility to infection from *U. virens*, *M. oryzae*, and *X. oryzae* pv. *oryzae* PXO99 (Figure 7D; Supplemental Figures S9 and S10B). In addition, expressing SCRE6^{C33A} in the Δ*scre6* mutant strain did not restore the virulence of *U. virens* (Figure 8A; Supplemental Figure S10A), and DEX-induced expression of SCRE6^{C33A} did not alter rice blast susceptibility in transgenic plants (Supplemental Figure S10B). Altogether, these results suggest that the phosphatase activity of SCRE6 is required for its virulence function.

Based on the above results, we propose a working model that illustrates how SCRE6 targets OsMPK6 to suppress host plant immunity (Figure 9). The PAMPs from phytopathogenic fungi are perceived by PRRs in plants, thus activating the intracellular MEKK1-MKK1-MPK6 cascade via the phosphorelay system (Rodriguez et al., 2010; Tang et al., 2017). As a negative regulator of plant immunity, OsMPK6 activation promotes its degradation via the ubiquitin proteasome system and thereby enhances plant immunity. During

U. virens infection, SCRE6 is secreted into plant cells and interacts with OsMPK6. Because SCRE6 functions as a tyrosine phosphatase to specifically dephosphorylate and stabilize OsMPK6, the enhanced accumulation of OsMPK6 attenuates plant immunity.

Although no SCRE6 homolog has been identified from other fungal species, it is both interesting and of practical relevance to investigate whether similar effector phosphatases harboring KIM motifs universally exist in fungal pathogens. Overall, we present here empirical evidence for fungal effectors that function as phosphatases to target immune-associated MAPKs so as to suppress host plant immunity.

Materials and methods

Plant material and microbial strains

The rice cultivar Nipponbare (NIP) was used as the wild type in this study. Rice plants were grown in a greenhouse for the pathogen inoculation assays. Rice seedlings were grown on plates with half-strength Murashige and Skoog (MS) medium in a growth chamber at 28°C under the white fluorescent light intensity of 200 μmol m^{-2} s^{-1}. The *U. virens* isolate P1 was used to generate the *scre6* knockout mutants. *Ustilaginoidea virens* was grown at 28°C on PSA medium (boiled extracts from 200 g of fresh potato, 20 g of sucrose, and 14-g agar per liter). The *M. oryzae* isolate Guy11 was
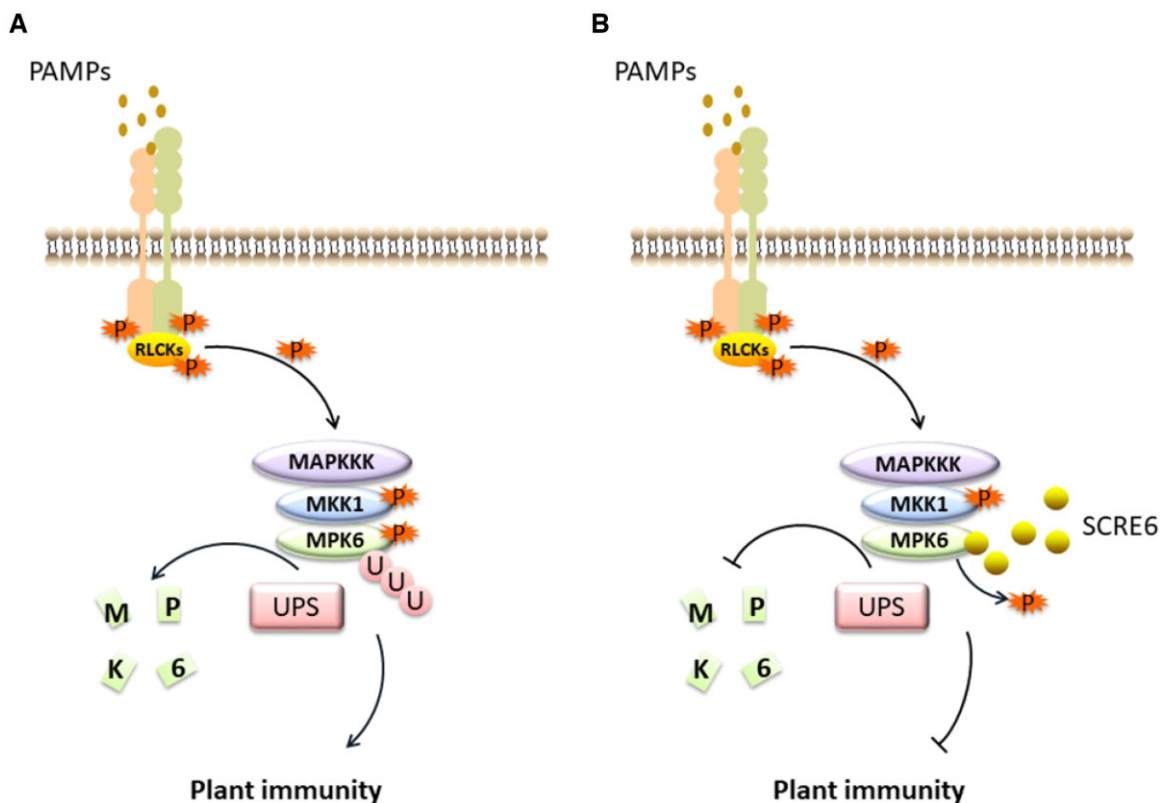
Figure 9 Working model illustrates how SCRE6 suppresses plant immunity by functioning as a tyrosine phosphatase. A, During the pathogen's infection of the host, PAMPs are recognized by PRRs in rice, thus activating intracellular OsMAPKKK–OsMKK1–OsMPK6 cascades through phosphorylation. Phosphorylated OsMPK6 is prone to being degraded via the 26S proteasome pathway, thereby enhancing host plant immunity. B, As a prerequisite effector, SCRE6 is secreted into plant cells during infection by *U. virens*. SCRE6 functions as a tyrosine phosphatase and dephosphorylates OsMPK6. The degradation of OsMPK6 is therefore inhibited and plant immunity is attenuated.

cultured on complete medium at 28°C. The *M. oryzae* isolate SZ4, obtained from the field, was grown on an oatmeal–tomato paste medium at 28°C in the dark. *Escherichia coli* strains were cultured on Luria–Bertani medium at 37°C and *X. oryzae* pv. *oryzae* PXO99 was cultured in nutrient broth at 28°C.

Yeast secretion assay

The yeast secretion assay was performed as described previously (Jacobs et al., 1997; Fang et al., 2016). Briefly, the putative SP-coding sequence of *SCRE6* was fused in frame with the *SUC2* gene lacking the SP-coding sequence. The pSUC2-*SCRE6(SP)* construct was then transformed into the yeast-invertase-deficient strain YTK12. The transformed YTK12 strain was cultured on CMD-W medium (0.67% [w/v] yeast N base, 0.075% [w/v] tryptophan drop-out supplement, 2% [w/v] sucrose, 0.1% [w/v] glucose, 2% [w/v] agar) and YPRAA medium (1% [w/v] yeast extract, 2% [w/v] peptone, 2% [w/v] raffinose, 2 µg L^{-1} antimycin A, 2% [w/v] agar).

Effector translocation assay

The open reading frame (ORF) of *SCRE6* was amplified and subcloned into the modified pYF11 vector containing the *RP27* promoter and GFP-coding sequences (Qi et al., 2016). Then the pYF11-*RP27pro:SCRE6-GFP* plasmid was transformed into *M. oryzae* Guy11 via PEG-mediated protoplast transformation (Yang et al., 2010). The expression of SCRE6-GFP in Guy11 was confirmed by fluorescence microscopy (Nikon Eclipse 90i). A conidial suspension (1×10^5 spores·mL^{-1}) of the transformed *M. oryzae* strain was injected, using a syringe, into the hollow interior of rice leaf sheaths. Inoculated leaf sheaths were incubated in a moist, dark chamber at 28°C. The inner epidermal layer was detached and observed at 30–36 h or 42–48 h post-inoculation via fluorescence microscopy for BIC or nucleus observations, respectively.

Plant transformations

The ORF of *SCRE6* was subcloned into pUC19-3 × FLAG-RBS. The *SCRE6* ORF together with the 3 × FLAG coding sequence was released by XhoI- and SpeI-mediated digestion and then re-ligated into pTA7001 for the generation of IE transgenic lines (Aoyama and Chua, 1997). *OsMPK6* cDNA was amplified and cloned into pC1305-pUbi to yield the *OsMPK6*-overexpressing lines. These constructs were transformed into *Agrobacterium tumefaciens* EHA105 via the freeze–thaw method (Weigel and Glazebrook, 2006). *Agrobacterium*-mediated rice transformation was performed as described previously (Li et al., 2015; Lu et al., 2015). Finally, to generate the hybrid, the IE transgenic lines and *OsMPK6*-overexpressing lines were crossed.

Ustilaginoidea transformation

A modified CRISPR/Cas9 (clustered regularly interspaced short palindromic repeats/CRISPR-associated protein 9) system was used to generate the *scre6* knockout mutants as described previously (Zheng et al., 2016). Briefly, the protoplasts were prepared by incubating the *U. virens* hyphae within a lysis solution (25-g L^{-1} Driselase, 10-g L^{-1} lysing enzyme, 0.05-g L^{-1} lyticase in 1.2 M KCl) for 3 h, at 28°C, with shaking (90 rpm). The protoplasts were collected through filtration, washed with an STC buffer (200-g L^{-1} sucrose, 0.05-M Tris–Cl, pH 8.0, 0.05-M $CaCl_2 \cdot 2H_2O$), and then re-suspended in STC to attain a concentration of 1.0×10^8 cells·mL^{-1}. Using fusion PCR, the hygromycin B phosphotransferase (*hph*) gene was fused into upstream and downstream DNA fragments of *SCRE6*. The gRNA primers were ligated into the pmCAS9-tRp vector. The pmCAS9-tRp-gRNA construct (5 µg) and the fusion PCR product (5 µg) were co-transformed into *U. virens* protoplasts as described by Li et al. (2019). The transformants were selected on a hygromycin B (100 µg·mL^{-1})-containing medium. Next, the coding sequence of *SCRE6* was amplified and subcloned into the pYP102 vector carrying the *RP27* promoter via in-fusion cloning (Vazyme; Zhou et al., 2018). The resulting construct was transformed into the Δ*scre6* mutant strains, using PEG-mediated transformation, to generate the complementation strains.

Southern blot analysis

Southern blot analysis was carried out as described previously (Li et al., 2019). For probe labeling and signal detection, the DIG High Prime DNA Labeling Kit and the Detection Starter Kit (Roche, Germany) were used according to the manufacturer's instructions.

Gene expression and MAPK activation assays

The wild-type and IE transgenic seedlings (1 week old) were pretreated with 10-µM DEX or a mock solution (0.03% ethanol [v/v]) for 16 h, and then immersed for 15 min in half-strength MS liquid medium (20-g sucrose and 2.2-g MS medium powder per liter, pH 5.6–5.8) containing 10 µg·mL^{-1} of chitin (Sigma, C9752) and 0.01% Silwet L-77 (GE Healthcare, Amersham, UK). The leaves were then collected for protein extractions. In vivo MAPK activation assays were implemented as previously described (Zhang et al., 2020). Briefly, total protein extracts were electrophoresed on 10% sodium dodecyl–sulfate (SDS)–polyacrylamide gels and blotted onto a polyvinylidene fluoride (PVDF) membrane. The blots were probed with an anti-p44/42 antibody (Cat# 9101, 1:2,000 dilution, Cell Signaling Technologies, Danvers, MA, USA) and also stained by Ponceau S for protein loading. The mock- and DEX-treated wild-type and IE transgenic seedlings were collected for total RNA extraction after undergoing the chitin treatment for 6 h, using an Ultrapure RNA extraction kit according to the manufacturer's instructions (CWBio, Beijing, China). Reverse transcription was performed to generate cDNA, with 2 µg of total RNA serving as the template, in the Reverse Transcription System (Takara, Dalian, China) using oligo-d(T)$_{18}$ as primers. The RT-qPCR was performed in a 20-µL reaction mixture consisting of 0.35 µL of cDNA, 0.2 mM of each gene-specific primer (Supplemental Data Set S1), and 2 × Maxima SYBR Green qPCR Master Mix, using an ABI PRISM 7500 Sequence Detection System (Applied Biosystems,

Carlsbad, CA, USA) as described previously (Fang et al., 2016). *OsActin* served as a reference gene. To detect gene expression in *U. virens*, five rice panicles were harvested at indicated days since inoculation and immediately frozen in liquid nitrogen. Five florets were randomly selected from each collected panicle for RNA isolation. The expression levels of *SCRE6* homologous genes were quantified via RT-qPCR, using α-tubulin as the internal reference gene.

Ustilaginoidea inoculation assay

The *U. virens* inoculation assay was performed as described previously (Han et al., 2015). Briefly, *U. virens* was cultured on PSA plates at 28°C for 10 days, and then transferred into PS liquid medium for 1 week with shaking (at 150 rpm). The culture of *U. virens* hyphae with conidia was smashed and diluted to 1×10^6 spores·mL^{-1} in PS medium. The conidial suspension was then injected into rice panicles at 5–7 days before the rice heading stage. At least 10 panicles were inoculated for each strain. False smut balls formed on rice panicles were counted at 4 weeks after inoculation.

Bacterial inoculation assay

The 6-week-old wild-type and IE transgenic plants were inoculated with *X. oryzae* pv. *oryzae* PXO99 using the leaf-clipping method (Kauffman et al., 1973; Wang et al., 2018). The wild-type and IE transgenic plants were sprayed with 30 μM of DEX or a mock solution at 24 h before inoculation. The leaf tip was cut using a pair of scissors that had been soaked in a suspension of *X. oryzae* pv. *oryzae* (optical density [OD]$_{600}$ = ~0.8). The lengths of disease lesions were measured at 12–14 days post-inoculation.

Magnaporthe oryzae inoculation and fungal biomass evaluation

The wild-type and IE transgenic seedlings (four-leaf stage) were spray-inoculated with the *M. oryzae* isolate SZ4. At 24 h before this inoculation, the seedlings had been sprayed with 30 μM of DEX or a mock solution. A conidial suspension (1×10^6 spores·mL^{-1}) containing 0.025% (v/v) Tween-20 was prepared for the inoculation. Disease symptoms on inoculated leaves were photographed at 7-day post-inoculation. Relative fungal biomass was quantified by measuring the expression level of the *M. oryzae* transposable element *MoPot2* through RT-qPCR. For this, *OsUBQ* was used as the internal reference gene.

Yeast two-hybrid assay

The coding sequence of *OsMPK6* was cloned into pGBKT7, and *SCRE6* or its homologous genes were cloned into pGADT7. The pair of pGADT7 and pGBKT7 constructs for each potential interaction was co-transformed into the yeast Gold strain using a Frozen-EZ Yeast Transformation II Kit (ZYMO RESEARCH). These yeast cells were grown for 3 days on a synthetic defined (SD) medium without Leu and Trp (SD/−Leu−Trp), and on a selective medium (SD/−His−Ade−Leu−Trp). The plasmid pGADT7-T was co-transformed with

pGBKT7-53 and pGBKT7-λ into yeast cells as the positive and negative controls, respectively.

LCI assay

The LCI assay was conducted as previously described (Chen et al., 2008). Briefly, the coding sequences of *OsMPK6* and *SCRE6* without their signal peptide-coding sequences were, respectively, subcloned into the vectors pCAMBIA1300-cLUC and pCAMBIA1300-nLUC. These constructs were transformed into the *A. tumefaciens* strain GV3101 using the freeze–thaw method (Weigel and Glazebrook, 2006). The constructed pCAMBIA1300-*cLUC-SCRE6* and pCAMBIA1300-*OsMPK6-nLUC* plasmids were agroinfiltrated into 4-week-old *N. benthamiana* leaves with an induction medium (10-mM MES, pH 5.6, 10-mM MgCl$_2$, and 150-mM acetosyringone). Luciferase activity was assessed at 72 h since agro-infiltration by spraying 1 mM of D-luciferin onto the infiltrated *N. benthamiana* leaves. The luminescence signals were captured by a CCD imaging apparatus (Berthold LB985).

The luciferase activity was quantified as described in Zhou et al. (2018). Briefly, leaf discs (0.6 cm in diameter) were punched from infiltrated leaf areas and these were placed in a 96-well plate containing 200 μL of sterile water. After replacing the sterile water with 200 μL of 1-mM D-luciferin, leaf discs were kept in the dark for 7 min. Luminescence was then quantified using a microplate reader (Tecan F200, Mannedorf, Switzerland) with an integration time of 0.5 s.

Co-IP assay

The coding sequences of *SCRE6* and *OsMPK6* were subcloned into pUC19-*35S-FLAG-RBS* and pUC19-*35S-HA-RBS*, respectively (Li et al., 2005). Rice protoplasts were prepared as described previously (He et al., 2016). The constructed vectors were co-transfected into rice protoplasts (2.5×10^6 cells·mL^{-1}) isolated from the wild-type seedlings (Li et al., 2015). Total proteins were extracted with an IP buffer (50-mM Tris–HCl, pH 7.4, 150-mM NaCl, 1-mM EDTA, 1% Triton X-100, and protease inhibitor cocktail) at 12 h after transfection. Total protein extracts were incubated with anti-FLAG M2 affinity beads (Sigma-Aldrich, A2220) at 4°C for 4 h. The beads were then rinsed five times with a pre-cooled 1× phosphate-buffered saline (PBS) buffer and the immunoprecipitates were eluted using 1× SDS–polyacrylamide gel electrophoresis (PAGE) loading buffer. The samples were subjected to immunoblot analyses using an HRP-conjugated anti-HA antibody (Roche, 11667475001, 1: 2,000 dilution) and an anti-FLAG antibody (Sigma-Aldrich, F1804, 1: 5,000 dilution).

In vitro protein expression and purification

The pGEX-4T-3 and pET30a vectors were respectively used for the expression of GST- and His-tagged proteins. The tagged proteins were expressed in *E. coli* BL21 (DE3) after induction by 0.1-mM isopropylthio-β-galactoside. His- and GST-tagged proteins were purified with Ni-NTA His·Bind and GST·Bind resins (Navogen, EMD Millipore, Billerica, MA,

USA), respectively, according to the manufacturer's instructions.

In vitro pulldown assay

In vitro purified His-OsMPK6 was incubated with glutathione agarose beads, in the presence of GST-SCRE6 or GST, for 3 h at 4°C. Then the beads were thoroughly washed with 1× PBS buffer. The proteins bound to the beads were eluted using 1× SDS–PAGE loading buffer and then subjected to immunoblot analyses employing anti-His (CWBIO, CW0285, 1: 5,000 dilution) and anti-GST (CWBIO, CW0084, 1: 5,000 dilution) antibodies.

Protein stability assay in protoplasts

The pUC19-*OsMPK6-HA* and pUC19-*GFP* constructs were co-transfected into rice protoplasts (2.5×10^6 cells·mL^{-1}) isolated from wild-type and IE transgenic seedlings. The protoplasts were incubated with 5-µM DEX or a mock solution (0.02% [v/v] ethanol) in the dark for 12 h, and then treated with the protein synthesis inhibitor CHX (50 µM). OsMPK6 abundance was detected at different elapsed times (0, 1, and 2 h) since the CHX treatment. *GFP* was co-expressed with pUC19-*OsMPK6-HA* to serve as an internal reference. Protein levels were determined by immunoblotting with horseradish peroxidase (HRP)-conjugated anti-HA (Roche, 11667475001, 1: 2,000 dilution), anti-FLAG (Sigma-Aldrich, F1804, 1: 5,000 dilution), and anti-GFP antibodies (CWBIO, CW0086, 1: 5,000 dilution).

Detection of OsMPK6 phosphorylation in vitro and in vivo

In vitro OsMPK6 phosphorylation was determined after the purified GST-OsMPK6 (1 µg) and GST-OsMKK1^{DD} (0.5 µg) were incubated with GST-SCRE6 (4 µg) or BSA (4 µg) in kinase assay buffer (100-mM Tris–HCl, pH 7.5, 100-mM MgCl$_2$, 100-mM MnCl$_2$, 10-mM DTT, 0.5-mM ATP, 1 µCi [λ^{32}P]ATP) for 1 h at 30°C (Xu et al., 2008). This reaction was stopped by adding 1× SDS–PAGE loading buffer. OsMPK6 phosphorylation was detected by autoradiography. The proteins were stained by Coomassie Brilliant Blue (CBB) for their loading.

The hybrid seedlings of *SCRE6-FLAG* IE and *OsMPK6-FLAG* transgenic plants were treated with DEX or a mock solution (0.03% [v/v] ethanol) for 16 h, followed by a chitin treatment for 15 min. Alternatively, rice protoplasts (2.5×10^6 cells·mL^{-1}) isolated from wild-type and IE transgenic seedlings were transfected with pUC19-*OsMPK6-FLAG* and were then incubated with 5 µM of DEX or a mock (0.02% [v/v] ethanol) solution for 12 h in the dark. The transfected protoplasts were treated with 10 µg·mL^{-1} of chitin or a mock solution for 10 min. Total proteins were extracted from the treated seedlings and transfected rice protoplasts with an IP buffer (50-mM Tris–HCl, pH 7.4, 150-mM NaCl, 1-mM EDTA, 1% Triton X-100, and protease inhibitor cocktail) and then subjected to immunoprecipitation using anti-FLAG M2 affinity beads (Sigma-Aldrich, A2220). The immunoprecipitated OsMPK6-FLAG and SCRE6-FLAG were detected with

an HRP-conjugated anti-FLAG antibody (Sigma-Aldrich, A8592). OsMPK6 phosphorylation in vivo was detected with an anti-p44/42 antibody (Cell Signaling Technologies, 9101, 1: 2,000 dilution). The β-actin was detected with an anti-actin antibody (CWBIO, CW0264, 1: 5,000 dilution).

In vitro dephosphorylation assay

GST-OsMPK6 (1 µg) was incubated with GST-OsMKK1^{DD} (0.5 µg) in the kinase assay buffer at 30°C for 1 h, after which EDTA (10 mM) was used to stop the reaction (Zhang et al., 2007). Purified GST-tagged SCRE6, SCRE2, UV_4984, UV_642, UV_2239, or BSA (4 µg) was individually added into the reaction mixture and these samples were further incubated for 30 min. The reaction was stopped by adding the 1× SDS–PAGE loading buffer. OsMPK6 phosphorylation was detected by autoradiography or by immunoblotting with an anti-p44/42 antibody. The proteins were stained by CBB for their loading.

OsMPK6 re-phosphorylation assay

After His-OsMPK6 was phosphorylated by GST-OsMKK1^{DD} as described above, 4 µg of GST-SCRE6 or 60 units of calf intestinal alkaline phosphatase (CIAP) was added into the reaction and incubated further (for 3 h). These samples were loaded onto GST·Bind resin to remove the GST-tagged proteins and the percolates were then loaded onto Ni-NTA His·Bind resin for the His-OsMPK6 enrichment. The eluted His-OsMPK6 was re-phosphorylated by GST-OsMKK1^{DD}, as described above. His-OsMPK6 phosphorylation was detected by immunoblotting with an anti-p44/42 antibody (Cell Signaling Technologies, 9101, 1: 2,000 dilution). The proteins were stained by CBB for their loading.

In vitro phosphatase assay

In vitro phosphatase assay was performed using the chromogenic *p*NPP as described by Yang et al. (2020). Various concentrations (0, 0.1, 0.2, and 0.4 µM) of GST-SCRE6, GST-SCRE2, GST-UV_4984, GST-UV_642, GST-UV_2239, or GST were incubated at 30°C, for 3 h, with 50 mM of *p*NPP (LABLEAD) in the phosphatase assay buffer (50-mM Tris–HCl, pH 7.5, 100-mM NaCl, 0.1-mM EDTA). The yellow product *p*-nitrophenol released from *p*NPP was determined by measuring the absorbance at 405 nm.

Mass spectrometry analysis

The phosphopeptide TETDLMpTEpYVVTR derived from the TEY motif of OsMPK6 was synthesized by Sangon Biotech (Shanghai, China). The phosphopeptide (0.1 µM) was incubated with 1 µM of SCRE6 and SCRE6^{C33A} in 200 µL of phosphatase assay buffer, at 30°C, for 1 h. After removing SCRE6 and SCRE6^{C33A} in an ultrafiltration filter device (10-kDa cutoff; Amicon, Sigma-Aldrich), the SCRE6-treated phosphopeptide was subjected to mass spectrometry that employed PRM.

Statistical analysis

Statistically significant differences among treatments were determined by a two-tailed Student's *t* test (*$P < 0.05$, **$P < 0.01$, and ***$P < 0.001$) using Microsoft Excel, or by one-way analysis of variance (ANOVA) followed by a least significant difference test (at $\alpha = 0.05$) using SPSS software (Supplemental Data Set 2).

Data and materials availability

All data needed to evaluate the conclusions in the article are present in the paper and/or the Supplementary Materials. Correspondence and requests for materials should be addressed to W.S.

Accession numbers

Sequence data for rice from this article can be found in the rice genome annotation project databases under the following accession numbers: OsMPK6 (Os10g0533600); OsMKK1 (Os06g0147800); OsMPK8 (Os01g0665200); OsMPK1 (Os06g0154500). Sequence data for *U. virens* from this article can be found in the GenBank data libraries under these accession numbers: SCRE6 (XP_042997324.1); UV_4984 (XP_042996714.1); UV_2239 (XP_042996128.1); and UV_642 (XP_043001606.1).

Supplemental data

The following materials are available in the online version of this article.

Supplemental Figure S1. Feature analysis for SCRE6 sequence and Southern blot analysis to confirm Δ*scre6* knockout mutants.

Supplemental Figure S2. OsMPK6 is phosphorylated by OsMKK1^{DD} in vitro.

Supplemental Figure S3. The degradation of OsMPK6-HA and OsMPK6^{DD}-HA is impeded by MG132 treatment.

Supplemental Figure S4. The expression of SCRE6-FLAG is induced by dexamethasone in different IE transgenic lines.

Supplemental Figure S5. SCRE6 is a phosphatase and dephosphorylates OsMPK6 in vitro.

Supplemental Figure S6. SCRE6 represents the prototype of a novel MAPK phosphatase family in *U. virens*.

Supplemental Figure S7. Expression patterns of *OsMPK6*, JA-, and SA-responsive genes in the wild-type and SCRE6-expressing transgenic plants.

Supplemental Figure S8. OsMPK6 overexpression results in enhanced disease susceptibility to *U. virens* in rice.

Supplemental Figure S9. Expression of SCRE6 in rice causes enhanced disease susceptibility to *U. virens* and bacterial blight diseases.

Supplemental Figure S10. Phosphatase activity of SCRE6 is required for its virulence function.

Supplemental Data Set 1. Primers were used in this study.

Supplemental Data Set 2. Data for all statistical analyses performed in this study.

References

Altschul SF, Madden TL, Schaffer AA, Zhang J, Zhang Z, Miller W, Lipman DJ (1997) Gapped BLAST and PSI-BLAST: a new generation of protein database search programs. Nucleic Acids Res **25**: 3389–3402

Aoyama T, Chua NH (1997) A glucocorticoid-mediated transcriptional induction system in transgenic plants. Plant J **11**: 605–612

Bartels S, Gonzalez BM, Lang D, Ulm R (2010) Emerging functions for plant MAP kinase phosphatases. Trends Plant Sci **15**: 322–329

Bhaskara GB, Wong MM, Verslues PE (2019) The flip side of phospho-signalling: regulation of protein dephosphorylation and the protein phosphatase 2Cs. Plant Cell Environ **42**: 2913–2930

Bhattacharjee S, Noor JJ, Gohain B, Gulabani H, Dnyaneshwar IK, Singla A (2015) Post-translational modifications in regulation of pathogen surveillance and signaling in plants: the inside- (and perturbations from) outside story. IUBMB Life **67**: 524–532

Bi G, Zhou Z, Wang W, Li L, Rao S, Wu Y, Zhang X, Menke F, Chen S, Zhou JM (2018) Receptor-like cytoplasmic kinases directly link diverse pattern recognition receptors to the activation of mitogen-activated protein kinase cascades in *Arabidopsis*. Plant Cell **30**: 1543–1561

Berriri S, Garcia AV, Frei DFN, Rozhon W, Pateyron S, Leonhardt N, Montillet JL, Leung J, Hirt H, Colcombet J (2012) Constitutively active mitogen-activated protein kinase versions reveal functions of *Arabidopsis* MPK4 in pathogen defense signaling. Plant Cell **24**: 4281–4293

Boevink PC, Wang X, McLellan H, He Q, Naqvi S, Armstrong MR, Zhang W, Hein I, Gilroy EM, Tian Z, et al. (2016) A *Phytophthora infestans* RXLR effector targets plant PP1c isoforms that promote late blight disease. Nat Commun **7**: 10311

Caunt CJ, Keyse SM (2013) Dual-specificity MAP kinase phosphatases (MKPs): shaping the outcome of MAP kinase signalling. FEBS J **280**: 489–504

Chen H, Zou Y, Shang Y, Lin H, Wang Y, Cai R, Tang X, Zhou JM (2008) Firefly luciferase complementation imaging assay for protein-protein interactions in plants. Plant Physiol **146**: 368–376

Espinosa A, Guo M, Tam VC, Fu ZQ, Alfano JR (2003) The *Pseudomonas syringae* type III-secreted protein HopPtoD2 possesses protein tyrosine phosphatase activity and suppresses programmed cell death in plants. Mol Microbiol **49**: 377–387

Fan J, Yang J, Wang YQ, Li GB, Li Y, Huang F, Wang WM (2016) Current understanding on *Villosiclava virens*, a unique flower-infecting fungus causing rice false smut disease. Mol Plant Pathol **17**: 1321–1330

Fang A, Gao H, Zhang N, Zheng X, Qiu S, Li Y, Zhou S, Cui F, Sun W (2019) A novel effector gene SCRE2 contributes to full virulence of *Ustilaginoidea virens* to rice. Front Immunol **10**: 845

Fang A, Han Y, Zhang N, Zhang M, Liu L, Li S, Lu F, Sun W (2016) Identification and characterization of plant cell death-inducing secreted proteins from *Ustilaginoidea virens*. Mol Plant Microbe Interact **29**: 405–416

Gao M, Liu J, Bi D, Zhang Z, Cheng F, Chen S, Zhang Y (2008) MEKK1, MKK1/MKK2 and MPK4 function together in a mitogen-activated protein kinase cascade to regulate innate immunity in plants. Cell Res **18**: 1190–1198

Gao X, Li Y, Fan J, Li L, Huang F, Wang WM (2012) Progress in the study of false smut disease in rice. J Agr Sci Technol **11**: 1211–1217

Han Y, Zhang K, Yang J, Zhang N, Fang A, Zhang Y, Liu Y, Chen Z, Hsiang T, Sun W (2015) Differential expression profiling of the early response to *Ustilaginoidea virens* between false smut resistant and susceptible rice varieties. BMC Genomics **16**: 955

He F, Chen S, Ning Y, Wang GL (2016) Rice (*Oryza sativa*) protoplast isolation and its application for transient expression analysis. Curr Opin Plant Biol **1**: 373–383

Hirt H (1997) Multiple roles of MAP kinases in plant signal transduction. Trends Plant Sci **2**: 11–15

Hunter T (1995) Protein kinases and phosphatases: the yin and yang of protein phosphorylation and signaling. Cell **80**: 225–236

Jacobs KA, Collins-Racie LA, Colbert M, Duckett M, Golden-Fleet M, Kelleher K, Kriz R, LaVallie ER, Merberg D, Spaulding V, et al. (1997) A genetic selection for isolating cDNAs encoding secreted proteins. Gene **198**: 289–296

Jiang C, Hei R, Yang Y, Zhang S, Wang Q, Wang W, Zhang Q, Yan M, Zhu G, Huang P, et al. (2020) An orphan protein of *Fusarium graminearum* modulates host immunity by mediating proteasomal degradation of TaSnRK1alpha. Nat Commun **11**: 4382

Jones JD, Dangl JL (2006) The plant immune system. Nature **444**: 323–329

Kauffman HE, Reddy A, Hsieh S, Merca SD (1973) Improved technique for evaluating resistance of rice varieties to *Xanthomonas oryzae*. Plant Dis Rep **57**: 537–541

Kerk D, Templeton G, Moorhead GB (2008) Evolutionary radiation pattern of novel protein phosphatases revealed by analysis of protein data from the completely sequenced genomes of humans, green algae, and higher plants. Plant Physiol **146**: 351–367

Keyse SM (2000) Protein phosphatases and the regulation of mitogen-activated protein kinase signalling. Curr Opin Plant Biol **12**: 186–192

Khang CH, Berruyer R, Giraldo MC, Kankanala P, Park SY, Czymmek K, Kang S, Valent B (2010) Translocation of *Magnaporthe oryzae* effectors into rice cells and their subsequent cell-to-cell movement. Plant Cell **22**: 1388–1403

Lee D, Lal NK, Lin ZD, Ma S, Liu J, Castro B, Toruno T, Dinesh-Kumar SP, Coaker G (2020) Regulation of reactive oxygen species during plant immunity through phosphorylation and ubiquitination of RBOHD. Nat Commun **11**: 1838

Letunic I, Bork P (2018) 20 years of the SMART protein domain annotation resource. Nucleic Acids Res **46**: D493–D496

Li S, Wang Y, Wang S, Fang A, Wang J, Liu L, Zhang K, Mao Y, Sun W (2015) The type III effector AvrBs2 in *Xanthomonas oryzae* pv. *oryzicola* suppresses rice immunity and promotes disease development. Mol Plant Microbe Interact **28**: 869–880

Li X, Lin H, Zhang W, Zou Y, Zhang J, Tang X, Zhou JM (2005) Flagellin induces innate immunity in nonhost interactions that is suppressed by *Pseudomonas syringae* effectors. Proc Natl Acad Sci USA **102**: 12990–12995

Li Y, Wang M, Liu Z, Zhang K, Cui F, Sun W (2019) Towards understanding the biosynthetic pathway for ustilaginoidin mycotoxins in *Ustilaginoidea virens*. Environ Microbiol **21**: 2629–2643

Liu S, Sun JP, Zhou B, Zhang ZY (2006) Structural basis of docking interactions between ERK2 and MAP kinase phosphatase 3. Proc Natl Acad Sci USA **103**: 5326–5331

Liu X, Zhou Y, Du M, Liang X, Fan F, Huang G, Zou Y, Bai J, Lu D (2022) The calcium-dependent protein kinase CPK28 is targeted by the ubiquitin ligases ATL31 and ATL6 for proteasome-mediated degradation to fine-tune immune signaling in *Arabidopsis*. Plant Cell **34**: 679–697

Lu F, Wang H, Wang S, Jiang W, Shan C, Li B, Yang J, Zhang S, Sun W (2015) Enhancement of innate immune system in monocot rice by transferring the dicotyledonous elongation factor Tu receptor EFR. J Integr Plant Biol **57**: 641–652

Luan S (2003) Protein phosphatases in plants. Annu Rev Plant Biol **54**: 63–92

Luo X, Wu W, Liang Y, Xu N, Wang Z, Zou H, Liu J (2020) Tyrosine phosphorylation of the lectin receptor-like kinase LORE regulates plant immunity. EMBO J **39**: e102856

Macho AP, Schwessinger B, Ntoukakis V, Brutus A, Segonzac C, Roy S, Kadota Y, Oh MH, Sklenar J, Derbyshire P, et al. (2014) A bacterial tyrosine phosphatase inhibits plant pattern recognition receptor activation. Science **343**: 1509–1512

Meng X, Zhang S (2013) MAPK cascades in plant disease resistance signaling. Annu Rev Phytopathol **51**: 245–266

Mithoe SC, Menke FL (2018) Regulation of pattern recognition receptor signalling by phosphorylation and ubiquitination. Curr Opin Plant Biol **45**: 162–170

Osada S (1995) Effect of false smut occurrence on yield and quality of rice *Ustilaginoidea virens*. Annu Rep Soc Plant Protect North Japan **46**: 30–32

Park CJ, Caddell DF, Ronald PC (2012) Protein phosphorylation in plant immunity: insights into the regulation of pattern recognition receptor-mediated signaling. Front Plant Sci **3**: 177

Qi Z, Liu M, Dong Y, Zhu Q, Li L, Li B, Yang J, Li Y, Ru Y, Zhang H, et al. (2016) The syntaxin protein (MoSyn8) mediates intracellular trafficking to regulate conidiogenesis and pathogenicity of rice blast fungus. New Phytol **209**: 1655–1667

Rafiqi M, Ellis JG, Ludowici VA, Hardham AR, Dodds PN (2012) Challenges and progress towards understanding the role of effectors in plant-fungal interactions. Curr Opin Plant Biol **15**: 477–482

Rodriguez MC, Petersen M, Mundy J (2010) Mitogen-activated protein kinase signaling in plants. Annu Rev Plant Biol **61**: 621–649

Shen X, Yuan B, Liu H, Li X, Xu C, Wang S (2010) Opposite functions of a rice mitogen-activated protein kinase during the process of resistance against *Xanthomonas oryzae*. Plant J **64**: 86–99

Shi Y (2009) Serine/threonine phosphatases: mechanism through structure. Cell **139**: 468–484

Soding J, Biegert A, Lupas AN (2005) The HHpred interactive server for protein homology detection and structure prediction. Nucleic Acids Res **33**: W244–W248

Song T, Zhang Y, Zhang Q, Zhang X, Shen D, Yu J, Yu M, Pan X, Cao H, Yong M, et al. (2021) The N-terminus of an *Ustilaginoidea virens* Ser-Thr-rich glycosylphosphatidylinositol-anchored protein elicits plant immunity as a MAMP. Nat Commun **12**: 2451

Sun W, Fan J, Fang A, Li Y, Tariqjaveed M, Li D, Hu D, Wang WM (2020) *Ustilaginoidea virens*: insights into an emerging rice pathogen. Annu Rev Phytopathol **58**: 363–385

Tang D, Wang G, Zhou JM (2017) Receptor kinases in plant-pathogen interactions: more than pattern recognition. Plant Cell **29**: 618–637

Tanaka S, Brefort T, Neidig N, Djamei A, Kahnt J, Vermerris W, Koenig S, Feussner K, Feussner I, Kahmann R (2014) A secreted *Ustilago maydis* effector promotes virulence by targeting anthocyanin biosynthesis in maize. eLife **3**: e1355

Tariqjaveed M, Mateen A, Wang S, Qiu S, Zheng X, Zhang J, Bhadauria V, Sun W (2021) Versatile effectors of phytopathogenic fungi target host immunity. J Integr Plant Biol **63**: 1856–1873

Tonks NK (2013) Protein tyrosine phosphatases-from housekeeping enzymes to master regulators of signal transduction. FEBS J 280: 346–378

Uhrig RG, Labandera A, Moorhead GB (2013) *Arabidopsis* PPP family of serine/threonine protein phosphatases: many targets but few engines. Trends Plant Sci 18: 505–513

Wang D, Wang H, Liu Q, Tu R, Zhou X, Zhang Y, Wu W, Yu P, Chen D, Zhan X, et al. (2021a) Reduction of OsMPK6 activity by a R89K mutation induces cell death and bacterial blight resistance in rice. Plant Cell Rep 40: 835–850

Wang J, Grubb LE, Wang J, Liang X, Li L, Gao C, Ma M, Feng F, Li M, Li L, et al. (2018) A regulatory module controlling homeostasis of a plant immune kinase. Mol Cell 69: 493–504

Wang J, Wang S, Hu K, Yang J, Xin X, Zhou W, Fan J, Cui F, Mou B, Zhang S, et al. (2018) The kinase OsCPK4 regulates a buffering mechanism that fine-tunes innate immunity. Plant Physiol 176: 1835–1849

Wang S, Li S, Wang J, Li Q, Xin XF, Zhou S, Wang Y, Li D, Xu J, Luo ZQ, et al. (2021b) A bacterial kinase phosphorylates OSK1 to suppress stomatal immunity in rice. Nat Commun 12: 5479

Weigel D, Glazebrook J (2006) Transformation of agrobacterium using the freeze-thaw method. CSH Protoc 2006: pdb.prot4666

Wu Y, Zhou JM (2013) Receptor-like kinases in plant innate immunity. J Integr Plant Biol 55: 1271–1286

Xing T, Ouellet T, Miki BL (2002) Towards genomic and proteomic studies of protein phosphorylation in plant-pathogen interactions. Trends Plant Sci 7: 224–230

Xu, J, Li, Y, Wang Y, Liu H, Lei L, Yang H, Liu G, Ren D (2008) Activation of MAPK kinase 9 induces ethylene and camalexin biosynthesis and enhances sensitivity to salt stress in *Arabidopsis*. J Biol Chem 283: 26996–27006

Yang J, Zhao X, Sun J, Kang Z, Ding S, Xu JR, Peng YL (2010) A novel protein Com1 is required for normal conidium morphology and full virulence in *Magnaporthe oryzae*. Mol Plant Microbe Interact 23: 112–123

Yang Z, Yang J, Wang Y, Wang F, Mao W, He Q, Xu J, Wu Z, Mao C (2020) Protein phosphatase 95 regulates phosphate homeostasis by affecting phosphate transporter trafficking in rice. Plant Cell 32: 740–757

Yuan B, Shen X, Li X, Xu C, Wang S (2007) Mitogen-activated protein kinase OsMPK6 negatively regulates rice disease resistance to bacterial pathogens. Planta 226: 953–960

Zhang J, Shao F, Li Y, Cui H, Chen L, Li H, Zou Y, Long C, Lan L, Chai J, et al. (2007) A *Pseudomonas syringae* effector inactivates MAPKs to suppress PAMP-induced immunity in plants. Cell Host Microbe 1: 175–185

Zhang K, Zhao Z, Zhang Z, Li Y, Li S, Yao N, Hsiang T, Sun W (2021) Insights into genomic evolution from the chromosomal and mitochondrial genomes of *Ustilaginoidea virens*. Phytopathol Res 3: 9

Zhang N, Yang J, Fang A, Wang J, Li D, Li Y, Wang S, Cui F, Yu J, Liu Y, et al. (2020) The essential effector SCRE1 in *Ustilaginoidea virens* suppresses rice immunity via a small peptide region. Mol Plant Pathol 21: 445–459

Zhang Y, Zhang K, Fang A, Han Y, Yang J, Xue M, Bao J, Hu D, Zhou B, Sun X, et al. (2014) Specific adaptation of *Ustilaginoidea virens* in occupying host florets revealed by comparative and functional genomics. Nat Commun 5: 3849

Zheng D, Wang Y, Han Y, Xu JR, Wang C (2016) UvHOG1 is important for hyphal growth and stress responses in the rice false smut fungus *Ustilaginoidea virens*. Sci Rep 6: 24824

Zhou W, Shi W, Xu XW, Li ZG, Yin CF, Peng JB, Pan S, Chen XL, Zhao WS, Zhang Y, et al. (2018) Glutamate synthase MoGlt1-mediated glutamate homeostasis is important for autophagy, virulence and conidiation in the rice blast fungus. Mol Plant Pathol 19: 564–578

Zhou Z, Bi G, Zhou JM (2018) Luciferase complementation assay for protein-protein interactions in plants. Curr Protoc Plant Biol 3: 42–50

Zipfel C (2014) Plant pattern-recognition receptors. Trends Immunol 35: 345–351